Newton flows for elliptic functions II

Structural stability: classification and representation

Helminck, G.F.; Twilt, F.

DOI
10.1007/s40879-017-0146-4

Publication date
2017

Document Version
Final published version

Published in
European Journal of Mathematics

European Journal of Mathematics (2017) 3:691–727
DOI 10.1007/s40879-017-0146-4

RESEARCH ARTICLE

Newton flows for elliptic functions II

Structural stability: classification and representation

Gerard F. Helminck[1] · **Frank Twilt**[2]

Received: 7 October 2016 / Accepted: 7 April 2017 / Published online: 25 May 2017

Abstract In our previous paper we associated to each non-constant elliptic function f on a torus T a dynamical system, the elliptic Newton flow corresponding to f. We characterized the functions for which these flows are structurally stable and showed a genericity result. In the present paper we focus on the classification and representation of these structurally stable flows. The phase portrait of a structurally stable elliptic Newton flow generates a connected, cellularly embedded graph $\mathcal{G}(f)$ on a torus T with r vertices, $2r$ edges and r faces that fulfil certain combinatorial properties (*Euler, Hall*) on some of its subgraphs. The graph $\mathcal{G}(f)$ determines the conjugacy class of the flow [*classification*]. A connected, cellularly embedded toroidal graph $\mathcal{G}$ with the above *Euler* and *Hall* properties, is called a *Newton graph*. Any Newton graph $\mathcal{G}$ can be realized as the graph $\mathcal{G}(f)$ of the structurally stable Newton flow for some function f. This leads to: up till conjugacy between flows and (topological) equivalency between graphs, there is a one to one correspondence between the structurally stable Newton flows and Newton graphs, both with respect to the same order r of the underlying functions f [*representation*]. Finally, we clarify the analogy between rational and elliptic Newton flows, and show that the detection of elliptic Newton flows is possible in polynomial time. The proofs of the above results rely on Peixoto's characterization/classification theorems for structurally stable dynamical systems on compact 2-dimensional manifolds, Stiemke's theorem of the alternatives, Hall's the-

✉ Gerard F. Helminck
g.f.helminck@uva.nl

Frank Twilt
f.twilt@kpnmail.nl

[1] Korteweg-de Vries Institute, University of Amsterdam, P.O. Box 94248, 1090 GE Amsterdam, The Netherlands

[2] Department of Applied Mathematics, University of Twente, P.O. Box 217, 7500 AE Enschede, The Netherlands

orem of distinct representatives, the Heffter–Edmonds–Ringer rotation principle for embedded graphs, an existence theorem on gradient dynamical systems by Smale, and an interpretation of Newton flows as steady streams.

Keywords Dynamical system (gradient-) · Desingularized Newton flow (rational, elliptic) · Structural stability · Elliptic function (Jacobian, Weierstrass) · Phase portrait · Newton graph (elliptic-, rational-) · Cellularly embedded toroidal (distinguished) graph · Face traversal procedure · Steady stream · Complexity · Angle property · Euler property · Hall condition

Mathematics Subject Classification 05C45 · 05C75 · 30C15 · 30D30 · 30F99 · 33E05 · 34D30 · 37C15 · 37C20 · 37C70 · 49M15 · 68Q25

1 Elliptic Newton flows: a recapitulation

In order to clarify the context of the present paper, we recapitulate some earlier results.

1.1 Elliptic Newton flows on the plane and on a torus

Let f be an elliptic (i.e., meromorphic, doubly periodic) function of order r $(\geqslant 2)$ on the complex plane $\mathbb{C}$ with (ω_1, ω_2), $\operatorname{Im} \omega_2/\omega_1 > 0$, as basic periods spanning a lattice Λ $(=\Lambda_{\omega_1,\omega_2})$.

The *planar elliptic Newton flow* $\overline{\mathcal{N}}(f)$ is a C^1-vector field on $\mathbb{C}$, defined as a *desingularized version*[1] of the planar dynamical system, $\mathcal{N}(f)$, given by (cf. [8])

$$\frac{dz}{dt} = \frac{-f(z)}{f'(z)}, \qquad z \in \mathbb{C}. \tag{1}$$

On a non-singular, oriented $\overline{\mathcal{N}}(f)$-trajectory $z(t)$ we have (cf. [8]):

– $\arg f$ = constant and $|f(z(t))|$ is a strictly decreasing function on t.

So that an $\overline{\mathcal{N}}(f)$-*equilibrium* is:

– attractor, or repellor, or saddle; see the comments on Fig. 1, where $N(f)$, $P(f)$ and $C(f)$ stand for, respectively, the set of zeros, poles and critical points for f.

Comments on Fig. 1:

Figure 1 (a), (b): In a k-fold zero (pole) for f the flow $\overline{\mathcal{N}}(f)$ exhibits a *stable* (*unstable*) *star node* and each (principal) value of $\arg f$ appears precisely k times on equally distributed incoming (outgoing) trajectories. Moreover, two different incoming (outgoing) trajectories intersect under a *non-vanishing* angle Δ/k, where Δ stands for the difference of the $\arg f$-values on these trajectories.

[1] In fact, we consider the system $dz/dt = -(1+|f(z)|^4)^{-1}|f'(z)|^2 f(z)/f'(z)$: a continuous version of Newton's damped iteration method for finding zeros for f.

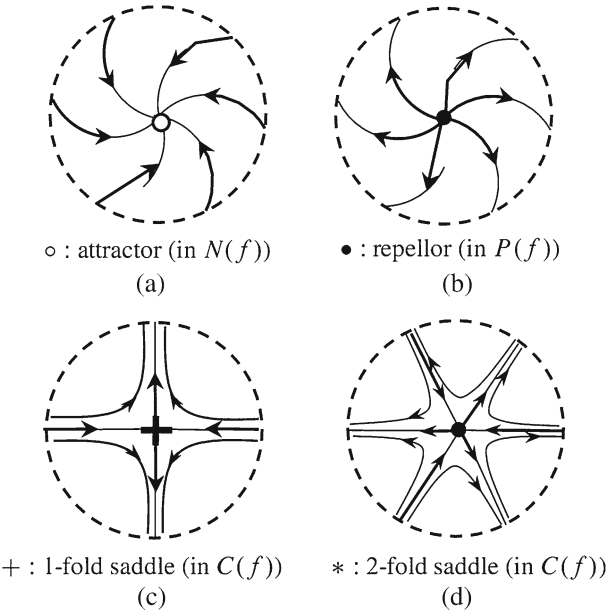

Fig. 1 Local phase portraits around equilibria of $\overline{\mathcal{N}}(f)$

Figure 1 (c), (d): In case of a k-fold critical point (i.e. a k-fold zero for f', no zero for f) the flow $\overline{\mathcal{N}}(f)$ exhibits a k-fold saddle, the stable (unstable) separatrices being equally distributed around this point. The two unstable (stable) separatrices at a onefold saddle, see Fig. 1 (c), constitute the "local" *unstable* (*stable*) *manifold* at this saddle point.

Functions of the type f correspond to the meromorphic functions on the complex torus $T(\Lambda)$ $(=\mathbb{C}/\Lambda_{\omega_1,\omega_2})$. So, we can interpret $\overline{\mathcal{N}}(f)$ as a global C^1-vector field, denoted[2] $\overline{\overline{\mathcal{N}}}(f)$, on the Riemann surface $T(\Lambda)$ and it is allowed to apply results for C^1-vector fields on compact differential manifolds, such as certain theorems of Poincaré–Bendixon–Schwartz on limiting sets and those of Baggis–Peixoto on C^1-structural stability. In particular, the local phase portraits around $\overline{\overline{\mathcal{N}}}(f)$-equilibria are as in Fig. 1.

1.2 The canonical form for a toroidal Newton flow; the topology τ_0

It is well known that the function f has precisely r zeros and r poles (counted by multiplicity) on the half open / half closed period parallelogram P $(=P_{\omega_1,\omega_2})$ given by $\{t_1\omega_1 + t_2\omega_2 : 0 \leqslant t_1 < 1,\ 0 \leqslant t_2 < 1\}$.

Denoting these zeros and poles by $a_1, \ldots, a_r$, respectively $b_1, \ldots, b_r$, we have (cf. [8,16]):

$$a_i \neq b_j, \quad i, j = 1, \ldots, r, \qquad \text{and} \qquad a_1 + \cdots + a_r = b_1 + \cdots + b_r \bmod \Lambda, \quad (2)$$

[2] Occasionally, we will refer to $\overline{\overline{\mathcal{N}}}(f)$ as to a *toroidal Newton flow*.

and thus

$$[a_i] \neq [b_j], \quad i, j = 1, \ldots, r, \qquad \text{and} \qquad [a_1] + \cdots + [a_r] = [b_1] + \cdots + [b_r], \quad (3)$$

where $[a_1], \ldots, [a_r]$ and $[b_1], \ldots, [b_r]$ are the zeros, respectively poles, for f on $T(\Lambda)$ and $[\cdot]$ stands for the congruency class mod Λ of a number in $\mathbb{C}$.

Theorem 1.1 (Canonical form for toroidal Newton flows)

- *Given a flow $\overline{\overline{\mathcal{N}}}(f)$ on $T(\Lambda)$, there exists an elliptic function f^* of order r with period lattice Λ^* $(=\Lambda_{1,i})$ together with a homeomorphism $T(\Lambda) \to T(\Lambda^*)$ mapping the phase portraits of $\overline{\overline{\mathcal{N}}}(f)$ and $\overline{\overline{\mathcal{N}}}(f^*)$ onto each other, thereby respecting the orientations of the trajectories.*
- *Moreover: If $a_1^*, \ldots, a_r^*$, respectively $b_1^*, \ldots, b_r^*$, are the zeros and poles of f^* in P^* $(=P_{1,i})$, then*

$$f^*(z) = \frac{\sigma(z - a_1^*) \cdots \sigma(z - a_r^*)}{\sigma(z - b_1^*) \cdots \sigma(z - b_{r-1}^*)\sigma(z - (b_r^*)')},$$
$$(b_r^*)' = a_1^* + \cdots + a_r^* - b_1^* - \cdots - b_{r-1}^*,$$

  where σ stands for the Weierstrass' sigma function w.r.t. the lattice Λ^*.
- *Conversely: if $c_1, \ldots, c_r$, respectively $d_1, \ldots, d_r$, stand for any pair of r tuples in P^* that fulfil relations (2), then due to the basic properties of the quasi periodic function σ, a function of the form*

$$\frac{\sigma(z - c_1) \cdots \sigma(z - c_r)}{\sigma(z - d_1) \cdots \sigma(z - d_{r-1})\sigma(z - d_r')},$$

  with $d_r' = c_1 + \cdots + c_r - d_1 - \cdots - d_{r-1}$, is elliptic w.r.t. to Λ^* with $[c_1], \ldots, [c_r]$, respectively $[d_1], \ldots, [d_r]$, as zeros, poles on $T(\Lambda^*)$.

Now, it is not difficult to see that the elliptic functions of order r, and also the underlying toroidal Newton flows, can be represented by the set of all ordered pairs

$$(\{[c_1], \ldots, [c_r]\}, \{[d_1], \ldots, [d_r]\})$$

of congruency classes mod Λ^* with $c_i, d_i \in P^*$, $i = 1, \ldots, r$, that fulfil (3). This representation space can be endowed with a topology, say τ_0, that is induced by the Euclidean topology on $\mathbb{C}$, and is natural in the following sense (cf. [8]): given an elliptic function f of order r and $\varepsilon > 0$ sufficiently small, there exists a τ_0-neighbourhood $\mathcal{O}$ of f such that for any $g \in \mathcal{O}$, the zeros (poles) for g are contained in ε-neighbourhoods of the zeros (poles) for f.

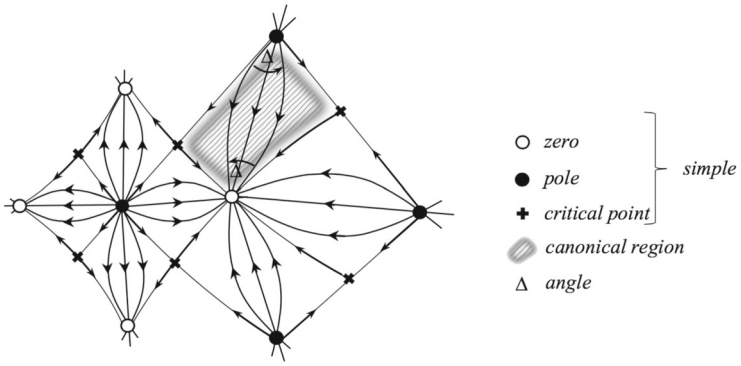

Fig. 2 Basin of repulsion (attraction) in the phase portrait of $\overline{\overline{\mathcal{N}}}(f)$ for a pole (zero) of f

1.3 Structural stability

Let $E_r(\Lambda)$ be the set of all elliptic functions f of order r on the torus $T(\Lambda) = \mathbb{C}/\Lambda$ and $N_r(\Lambda)$ the set of all toroidal Newton flows $\overline{\overline{\mathcal{N}}}(f)$. We assume (no loss of generality; see Sect. 1.2) that $\Lambda = \Lambda_{1,i}$, and write $E_r(\Lambda) = E_r$, $T(\Lambda) = T$ and $N_r(\Lambda) = N_r$.

By $X(T)$ we mean the set of all C^1-vector fields on T, endowed with the C^1-topology. The topology τ_0 on E_r and the C^1-topology on $X(T)$ are matched by (cf. [8]):

Lemma 1.2 *The map* $E_r \to X(T)\colon f \mapsto \overline{\overline{\mathcal{N}}}(f)$ *is* τ_0-C^1-*continuous.*

Two flows $\overline{\overline{\mathcal{N}}}(f)$ and $\overline{\overline{\mathcal{N}}}(g)$ in N_r are called *conjugate*, denoted $\overline{\overline{\mathcal{N}}}(f) \sim \overline{\overline{\mathcal{N}}}(g)$, if there is a homeomorphism from T onto itself mapping maximal trajectories of $\overline{\overline{\mathcal{N}}}(f)$ onto those of $\overline{\overline{\mathcal{N}}}(g)$, thereby respecting the orientations of these trajectories.

We call the flow $\overline{\overline{\mathcal{N}}}(f)$ τ_0-*structurally stable*, if there is a τ_0-neighborhood $\mathcal{O}$ of f such that for all $g \in \mathcal{O}$ we have $\overline{\overline{\mathcal{N}}}(f) \sim \overline{\overline{\mathcal{N}}}(g)$. The set of all structurally stable Newton flows $\overline{\overline{\mathcal{N}}}(f)$ is denoted by $\widetilde{N}_r$.

By Lemma 1.2, it follows that C^1-structural stability for $\overline{\overline{\mathcal{N}}}(f)$ implies τ_0-structural stability for $\overline{\overline{\mathcal{N}}}(f)$. So, when discussing structural stable toroidal Newton flows we will skip the adjectives τ_0 and C^1. We proved (cf. [8]):

Theorem 1.3 (Characterization and genericity of structural stability)

(I) $\overline{\overline{\mathcal{N}}}(f) \in \widetilde{N}_r$ *if and only if the function* f *is non-degenerate, i.e., all zeros, poles and critical points for* f *are simple, and no critical points for* f *are connected by* $\overline{\overline{\mathcal{N}}}(f)$*-trajectories.*

(II) *The set of all non-degenerate functions of order* r *is open and dense in* E_r.

We list some properties that will play a role in the sequel, see the comments on Fig. 1:

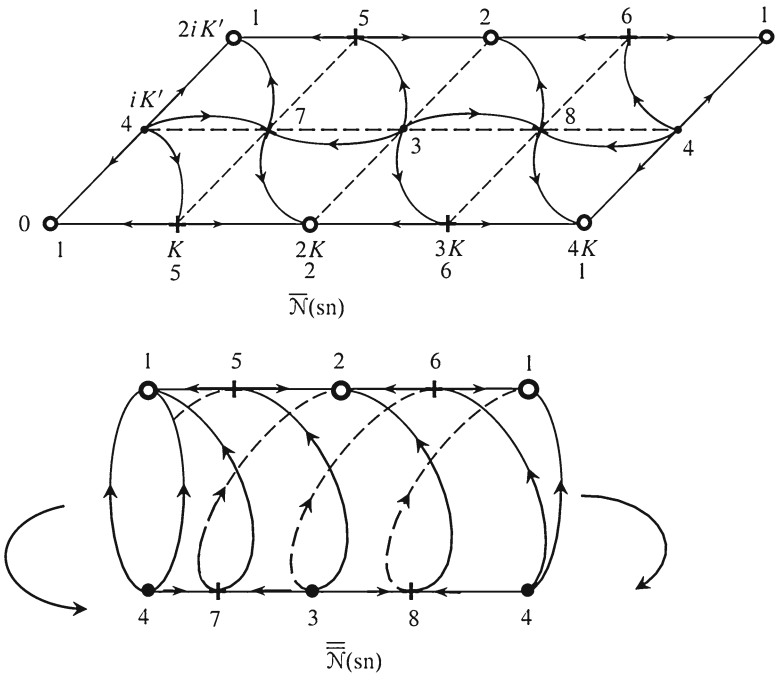

Fig. 3 Planar and toroidal Newton flows for $\mathrm{sn}_{\omega_1,\omega_2}$; structurally stable

Lemma 1.4 (Properties of structurally stable toroidal Newton flows $\overline{\overline{\mathcal{N}}}(f)$)

(a) *If* $\overline{\overline{\mathcal{N}}}(f)$ *is structurally stable, then also* $\overline{\overline{\mathcal{N}}}(1/f)$ *is, and* $\overline{\overline{\mathcal{N}}}(1/f) = -\overline{\overline{\mathcal{N}}}(f)$. [Duality]

(b) *There are precisely* $2r$ *orthogonal saddles for* $\overline{\overline{\mathcal{N}}}(f)$.

(c) *The boundary of the basin of a repellor* (*attractor*) *is made up by the unstable* (*stable*) *manifolds at the saddles situated in this boundary* (*cf. Fig. 2*).

As an illustration we present in Figs. 3 and 4 planar/toroidal Newton flows for Jacobian functions $\mathrm{sn}_{\omega_1,\omega_2}$ with only simple attractors, repellors and saddles; see also [1,8] and the forthcoming Remark 2.15. For more examples of (structurally stable) Newton flows, see [9].

1.4 Toroidal versus rational Newton flows; purpose of the paper

If we choose for f *rational* functions (meromorphic on the Riemann sphere S^2), we obtain the class of so-called *spherical Newton flows*. These flows have many concepts/features in common with (the class of) toroidal Newton flows and are already studied before (cf. [10–13]); in fact, *characterization* and *genericity results*, analogous to Theorem 1.3, have been proved. Moreover, spherical Newton flows can be *classified* and *represented* in terms of certain sphere graphs (i.e. the "principal parts" of the phase

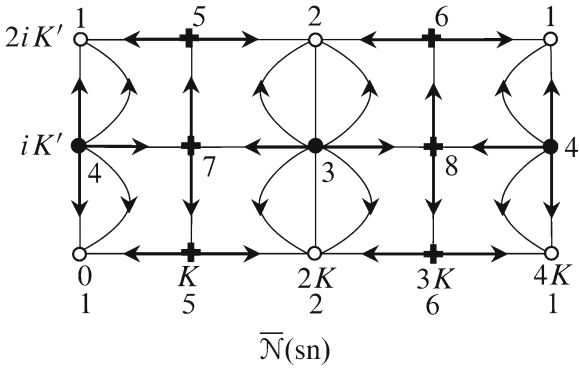

Fig. 4 Planar Newton flow for $\mathrm{sn}_{\omega_1,\omega_2}$; not structurally stable

portraits of structurally stable spherical Newton flows). The target of the present paper is to prove such a *classification* and *representation result* for toroidal Newton flows.

2 Structurally stable elliptic Newton flows: classification

In this section, let f be non-degenerate of order r, thus $\overline{\overline{\mathcal{N}}}(f)$ is structurally stable. Then, the following definition makes sense: (cf. Sect. 1.1, Lemma 1.4).

Definition 2.1 The graph $\mathcal{G}(f)$, $f \in \widetilde{E}_r$, on the torus T is given by:

- Vertices are the r zeros for f on T (as attractors for $\overline{\overline{\mathcal{N}}}(f)$).
- Edges are the $2r$ unstable manifolds at the critical points for f on T as $\overline{\overline{\mathcal{N}}}(f)$-saddles.

Note that the faces of $\mathcal{G}(f)$ are precisely the r *basins of repulsion* of the poles, say $[b_j]$, $j = 1, \ldots, r$, for f on T (as repellors for $\overline{\overline{\mathcal{N}}}(f)$) and will be denoted by $F_{b_j}(f)$; their boundaries by $\partial F_{b_j}(f)$. These boundaries, consisting of *unstable manifolds* at saddles for $\overline{\overline{\mathcal{N}}}(f)$, are subgraphs of $\mathcal{G}(f)$, see Fig. 2.

Analogously, we define the graph,[3] say $\mathcal{G}^*(f)$, on the poles and the stable $\overline{\overline{\mathcal{N}}}(f)$-manifolds at the critical points for f on T.

Lemma 2.2 *Both $\mathcal{G}(f)$ and $\mathcal{G}^*(f)$ are multigraphs*[4] *embedded in T.*

Proof If $\mathcal{G}(f)$ would have a loop, the two unstable $\overline{\overline{\mathcal{N}}}(f)$-separatrices at some critical point for f would approach the same zero, say $[a]$, on T. In that case, the zeros (simple!) for f in the plane, corresponding to $[a]$, will be approached by two *different* trajectories (of the planar version $\overline{\mathcal{N}}(f)$) with the same value of $\arg f$. This is impossible (cf. the comments on Fig. 1). The second part of the assertion follows by interchanging the roles of the poles and zeros for f. □

[3] $\mathcal{G}(f)$ and $\mathcal{G}^*(f)$ are *geometrical duals*; see also Sect. 3.

[4] i.e., multiple edges are allowed, but no loops (cf. [6]); note however that the concept of multigraph in [18] includes loops.

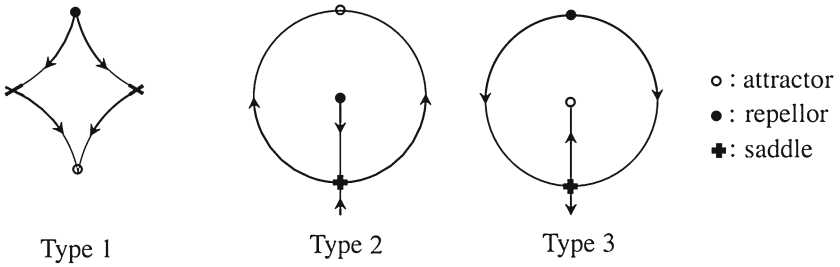

Fig. 5 The canonical regions of a structural stable flow on T

Corollary 2.3 *An edge in $\mathcal{G}(f)$ or $\mathcal{G}^*(f)$ is contained in the boundaries of two different faces.*

Next we introduce a graph on T, denoted $\mathcal{G}(f) \wedge \mathcal{G}^*(f)$, which may be considered as the "common refinement of $\mathcal{G}(f)$ and $\mathcal{G}^*(f)$".

Definition 2.4 The *vertices* of $\mathcal{G}(f) \wedge \mathcal{G}^*(f)$ are defined as the zeros, poles and critical points for f, whereas the *edges* are the stable and unstable separatrices of $\overline{\overline{\mathcal{N}}}(f)$ at the critical points for f.

The faces of $\mathcal{G}(f) \wedge \mathcal{G}^*(f)$ are the so-called *canonical regions* for $\overline{\overline{\mathcal{N}}}(f)$, i.e. the connected components of what is left after deleting from T all the $\overline{\overline{\mathcal{N}}}(f)$-equilibria and all stable and unstable manifolds at the saddles of $\overline{\overline{\mathcal{N}}}(f)$. A priori, the canonical regions of a C^1-structurally stable flow on T (without closed orbits) are of one of the Types 1, 2, 3 in Fig. 5 (cf. Fig. 2, [20]). However, by Lemma 2.2 the flow $\overline{\overline{\mathcal{N}}}(f)$—although structurally stable—cannot admit canonical regions of Types 2 and 3.

So, we only have to deal with canonical regions of Type 1. Since all zeros, poles and critical points for f are simple, we find (see Sect. 1.1):

Lemma 2.5 *In a canonical region of $\overline{\overline{\mathcal{N}}}(f)$, the angles (anti-clockwise measured) at the pole and the zero are well defined, strictly positive and equal.*

Since a face $F_{b_j}(f)$ is built up from all canonical regions that have $[b_j]$ in common, we find:

Corollary 2.6 *All (anti-clockwise measured) angles spanning a sector of $F_{b_j}(f)$ at the vertices in its boundary, are non-vanishing and sum up to 2π.*

Lemma 2.7 *Each subgraph $\partial F_{b_j}(f)$ is Eulerian.*[5]

Proof Traverse the set of all canonical regions centered at $[b_j]$ once. In this way we determine a closed walk, say w_{b_j}, through all the vertices and edges of $\partial F_{b_j}(f)$; see Fig. 6. By Corollary 2.3, this walk contains each edge of $\partial F_{b_j}(f)$ only once (since otherwise the two stable separatrices at the saddle on such an edge must originate from $[b_j]$). So, w_{b_j} is the desired Euler trail. □

[5] i.e. the graph $\partial F_{b_j}(f)$ admits a so-called *Euler trail*: a closed walk that traverses each edge exactly once and goes through all vertices. We do not distinguish between an Euler trail and its cyclic shift.

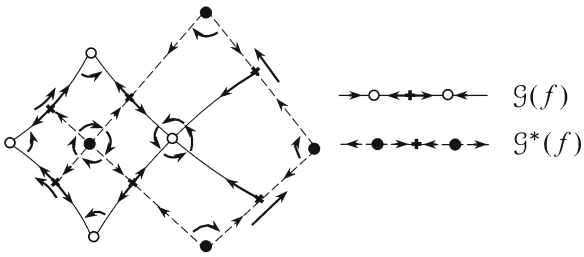

Fig. 6 Oriented facial walks on $\mathcal{G}(f)$ and $\mathcal{G}^*(f)$

The walk w_{b_j} in the above proof will be referred to as to the *facial walk* for $\partial F_{b_j}(f)$. Analogously, we define the (Eulerian!) facial walks on the boundaries of the $\mathcal{G}^*(f)$-faces (i.e., the *basins of attraction* of the zeros, say $[a_i]$, $i = 1, \ldots, r$, for f on T as attractors for the Newton flow $\overline{\overline{\mathcal{N}}}(f)$).

Remark 2.8 Note that in these facial walks the same vertex may occur more than once. However, by Lemma 2.2, a vertex in a facial walk cannot be adjacent to itself.

The orientations of $\mathcal{G}(f)$ and $\mathcal{G}^*(f)$:
We endow (the faces of) $\mathcal{G}(f)$ with a coherent orientation as follows: for each facial walk we demand that the (constant) values of $\arg f(z)$ on consecutive edges form an increasing sequence. This is imposed by the anti-clockwise ordering of the $\mathcal{G}(f)$-edges around a common vertex, which on its turn induces clockwise orientations of the $\mathcal{G}^*(f)$-edges incident to a given vertex. This leads to an orientation of (the facial walks on) $\mathcal{G}^*(f)$ which is opposite to the orientation of $\mathcal{G}(f)$ as chosen before; see Fig. 6. From now on we assume that all graphs $\mathcal{G}(f)$ and $\mathcal{G}^*(f)$, $f \in \widetilde{E}_r$, are oriented in this way: $\mathcal{G}(f)$ always clockwise; $\mathcal{G}^*(f)$ always anti-clockwise. By $-\mathcal{G}(f)$ we mean $\mathcal{G}(f)$ with anti-clockwise orientation and by $-\mathcal{G}^*(f)$ the clockwise oriented graph $\mathcal{G}^*(f)$.

Lemma 2.9 *The (multi)graphs $\mathcal{G}(f)$ and $\mathcal{G}^*(f)$ are connected and cellularly embedded.*[6]

Proof We focus on $\mathcal{G}(f)$ and follow the treatise [18] closely. Consider the r facial walks w_{b_j} and put $l_j = \text{length } w_{b_j}$. Consider for each w_{b_j} a so-called *facial polygon*, i.e. a polygon in the plane with l_j sides labelled by the edges of $\partial F_{b_j}(f)$ (taking the orientation of w_{b_j} into account), so that each polygon is disjoint from the other polygons. Now we take all facial polygons. Each $\mathcal{G}(f)$-edge occurs precisely once in two different facial walks and this determines orientations of the sides of the polygons. By identifying each side with its mate, we construct (cf. [18]) an orientable, connected surface S, homeomorphic to T, and (in S) a 2-cell embedded graph, which is—up to an isomorphism—equal to $\mathcal{G}(f)$. By Euler's formula for graphs on T (cf. [5]), $\mathcal{G}(f)$ is connected and orientable as well. Finally, we note that a 2-cell embedding is always cellular (cf. [18]). □

[6] i.e. each face is homeomorphic to an *open* disk in $\mathbb{R}^2$.

The *abstract directed graph*, underlying $\mathcal{G}(f) \wedge \mathcal{G}^*(f)$, will be denoted by $\mathbb{P}(f)$, where the directions are induced by the orientations of the (un)stable separatrices at $\overline{\overline{\mathcal{N}}}(f)$-saddles. Each canonical region is represented by a quadruple of directed edges in $\mathbb{P}(f)$, and is associated with precisely one pole, one zero (in opposite position) and two critical points for f on T. Following Peixoto [19,20], such a quadruple is called a *distinguished set* (of Type 1). The graph $\mathbb{P}(f)$ together with the collection of all distinguished sets is denoted by $\mathbb{P}^{\mathrm{d}}(f)$. We say "$\mathbb{P}^{\mathrm{d}}(f)$ is realized by the distinguished graph of $\overline{\overline{\mathcal{N}}}(f)$ on T".

We need a classical result due to Peixoto (cf. [20]) on structurally, C^1-stable vector fields on 2-dimensional compact manifolds. In the context of our elliptic Newton flows this yields (together with Lemma 1.2): if $f, h \in \widetilde{E}_r$, then

$$\overline{\overline{\mathcal{N}}}(f) \sim \overline{\overline{\mathcal{N}}}(h) \iff \mathbb{P}^{\mathrm{d}}(f) \sim \mathbb{P}^{\mathrm{d}}(h). \tag{4}$$

Here, $\sim$ in the l.h.s stands for "conjugacy" and $\sim$ in the r.h.s. for *isomorphism between* $\mathbb{P}^{\mathrm{d}}(f)$ and $\mathbb{P}^{\mathrm{d}}(h)$ (as directed abstract graphs), preserving the distinguished sets and respecting the cyclic ordering (induced by the embedding in T) of the distinguished sets around a common vertex.

Theorem 2.10 (Classification of structurally stable elliptic Newton flows by graphs) *Let $\overline{\overline{\mathcal{N}}}(f)$ and $\overline{\overline{\mathcal{N}}}(h)$ be structurally stable (thus $f, h \in \widetilde{E}_r$), then*

$$\overline{\overline{\mathcal{N}}}(f) \sim \overline{\overline{\mathcal{N}}}(h) \iff \mathcal{G}(f) \sim \mathcal{G}(h) \ \ (\textit{and thus also } \mathcal{G}^*(f) \sim \mathcal{G}^*(h)),$$

where $\sim$ in the r.h.s. stands for equivalency between the oriented graphs (i.e., an isomorphism respecting their orientations).

Proof Apply (4) to $\overline{\overline{\mathcal{N}}}(f)$ and $\overline{\overline{\mathcal{N}}}(h)$. □

The graph $\mathcal{G}(1/f)$ is also well defined (with as faces $F_{a_i}(1/f)$) and associated with the structurally stable flow $\overline{\overline{\mathcal{N}}}(1/f)$ $(= -\overline{\overline{\mathcal{N}}}(f))$. The flow $\overline{\overline{\mathcal{N}}}(1/f)$ is the dual version of $\overline{\overline{\mathcal{N}}}(f)$, i.e., $\overline{\overline{\mathcal{N}}}(1/f)$ is obtained from $\overline{\overline{\mathcal{N}}}(f)$ by reversing the orientations of the trajectories of the latter flow, thereby changing repellors into attractors and vice versa. Clearly, $\mathcal{G}(1/f)$ and $\mathcal{G}^*(f)$ coincide, be it with opposite orientations, i.e., $\mathcal{G}(1/f) = -\mathcal{G}^*(f)$, where, due to our convention on orientations, $\mathcal{G}(1/f)$ is clockwise oriented. Also, we have $\mathcal{G}(f) = -\mathcal{G}^*(1/f)$.

Note that, in general, $\overline{\overline{\mathcal{N}}}(f)$ and $\overline{\overline{\mathcal{N}}}(1/f)$ are *not* conjugate. In the special case where $\overline{\overline{\mathcal{N}}}(f) \sim \overline{\overline{\mathcal{N}}}(1/f)$ we call these flows *self-dual*, and we have (Theorem 2.10)

$$\overline{\overline{\mathcal{N}}}(f) \sim \overline{\overline{\mathcal{N}}}\left(\frac{1}{f}\right) \iff \mathcal{G}(f) \sim \mathcal{G}\left(\frac{1}{f}\right) \iff \mathcal{G}(f) \sim -\mathcal{G}^*(f).$$

If $\mathcal{G}(f) \sim -\mathcal{G}^*(f)$ holds, we call $\mathcal{G}(f)$ and $\mathcal{G}^*(f)$ *self-dual*.

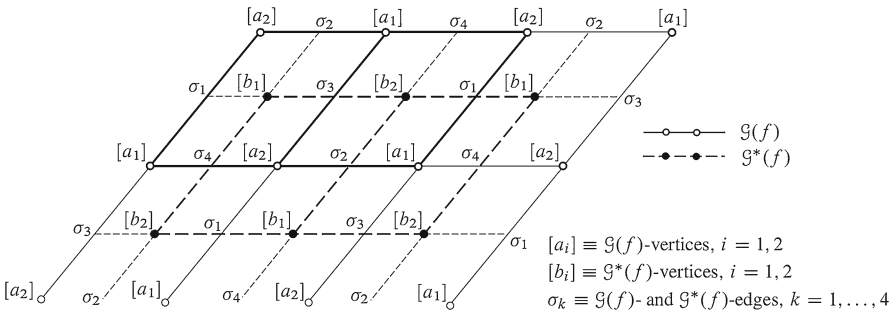

Fig. 7 The graphs $\mathcal{G}(f)$ and $\mathcal{G}^*(f)$, $f \in \widetilde{E}_2$

Remark 2.11 (*On the classification under conjugacy and duality*) Conjugate flows are considered as equal. Although, in general, $\overline{\overline{\mathcal{N}}}(f)$ and $\overline{\overline{\mathcal{N}}}(1/f)$ are not conjugate, it is reasonable to consider also these flows, being related by a trivial (but orientation reversing) identity, as "equal". See our paper [9].

Remark 2.12 (*On self-duality*) If $\overline{\overline{\mathcal{N}}}(f)$ is self-dual and conjugate with $\overline{\overline{\mathcal{N}}}(h)$, then $\overline{\overline{\mathcal{N}}}(h)$ is also self-dual.

Corollary 2.13 *Any two structurally stable 2nd order elliptic Newton flows are conjugate. In particular, these flows are self-dual.*

Proof Let $\overline{\overline{\mathcal{N}}}(f)$, $f \in \widetilde{E}_2$, be chosen arbitrarily. By Corollary 2.3, the two faces of $\mathcal{G}(f)$ share their boundaries. So, the common facial walk w_f of these faces is built up from the four $\mathcal{G}(f)$-edges and the two $\mathcal{G}(f)$-vertices (each appearing twice but not consecutive!). Hence, compare the construction in the proof of Lemma 2.9 and see Fig. 7, $\mathcal{G}(f)$ is determined by the anti-clockwise oriented walk w_f. The same holds for any other flow $\overline{\overline{\mathcal{N}}}(h)$ with facial walk w_h, $h \in \widetilde{E}_2$. Apparently, w_f and w_h maybe considered as equal, under a suitably chosen relabeling of their vertices and edges. Hence $\mathcal{G}(f) \sim \mathcal{G}(h)$ and thus $\overline{\overline{\mathcal{N}}}(f) \sim \overline{\overline{\mathcal{N}}}(h)$. In particular, put $h = 1/f$, then we find $\mathcal{G}(f) \sim \mathcal{G}(1/f)$, compare Fig. 7 and Remark 2.12. □

Remark 2.14 For basically the same proof of Corollary 2.13, see [22].

Remark 2.15 The flow $\overline{\overline{\mathcal{N}}}(\mathrm{sn})$, in the non-rectangular case (cf. Fig. 3) exhibits an example of a 2nd order structurally stable elliptic Newton flow. By Corollary 2.13, this is the only possibility (up to conjugacy) for a flow in $\widetilde{\mathcal{N}}_2$. Note that the flow in Fig. 4 (rectangular case) is not structurally stable (because of the saddle connections).

We proceed by introducing flows that are closely related to $\mathcal{N}(f)$, $\overline{\mathcal{N}}(f)$ and $\overline{\overline{\mathcal{N}}}(f)$: the so-called *rotated Newton flows*.

Definition 2.16 For $f \in E_r$, let $\mathcal{N}^{\perp}(f)$ be a dynamical system of the type

$$\frac{dz}{dt} = \frac{-if(z)}{f'(z)}.$$

Apparently, $\mathcal{N}^{\perp}(f)(=i\mathcal{N}(f))$ is a complex analytic vector field outside the set $C(f)$ of critical points for f. As in Sect. 1.1, we turn $\mathcal{N}^{\perp}(f)$ into a C^1-system on the whole plane with (on $\mathbb{C}\backslash C(f)$) the same phase portrait as $\mathcal{N}^{\perp}(f)$ by $\overline{\mathcal{N}}^{\perp}(f) = i\overline{\mathcal{N}}(f)$. The function f, being elliptic, the system $\overline{\mathcal{N}}^{\perp}(f)$ can be interpreted as a C^1-flow on T and as such it will be referred to as to $\overline{\overline{\mathcal{N}}}^{\perp}(f)$, in particular,

$$\overline{\overline{\mathcal{N}}}^{\perp}(f) \text{ is of the class } C^1, \text{ and } \overline{\overline{\mathcal{N}}}^{\perp}\left(\frac{1}{f}\right) = -\overline{\overline{\mathcal{N}}}^{\perp}(f).$$

Lemma 2.17 *Let $z^{\perp}(t)$ be the (maximal) $\mathcal{N}^{\perp}(f)$-trajectory through a non-equilibrium $\check{z} = z^{\perp}(0)$, then:*

(i) $f(z^{\perp}(t)) = e^{-it} f(\check{z})$ [*thus* $|f(z^{\perp}(t))| =$ constant $(\neq 0)$].

(ii) *A zero or pole for f is a center for $\mathcal{N}^{\perp}(f)$* [*thus also for $\overline{\mathcal{N}}^{\perp}(f)$, $\overline{\overline{\mathcal{N}}}^{\perp}(f)$*].

(iii) *A k-fold critical point for f is a k-fold saddle for $\overline{\mathcal{N}}^{\perp}(f)$* [*thus also for $\overline{\overline{\mathcal{N}}}^{\perp}(f)$*].

Proof Assertions (i) and (iii): use $\mathcal{N}^{\perp}(f) = i\mathcal{N}(f)$. Note that outside $N(f) \cup P(f)$ the flow $\mathcal{N}^{\perp}(f)$ can be considered as the Newton flow for $h(z) = \exp(-i \log f(z))$. For assertion (ii): let z_0 be a zero or pole for f with multiplicity k, thus an isolated zero for $\mathcal{N}^{\perp}(f)$. In a neighborhood of z_0, system $\mathcal{N}^{\perp}(f)$ is linearly approximated by

$$\frac{dz}{dt} = \frac{-i(z - z_0)}{k}.$$

Thus z_0 is a non-degenerate equilibrium for $\mathcal{N}^{\perp}(f)$ with characteristic roots $\pm i/k$. By the first assertion in the lemma, a regular integral curve through a point $\check{z}$ close to z_0, but $\neq z_0$, cannot end up at or leave from z_0. Hence, this point is neither a focus, nor a centro-focus for $\mathcal{N}^{\perp}(f)$ (cf. [2]) and must be a center for $\mathcal{N}^{\perp}(f)$. □

In view of the above assertion (i), a closed orbit for $\overline{\overline{\mathcal{N}}}^{\perp}(f)$ cannot be a limit cycle, and (by (ii)) a separatrix $z^{\perp}(t)$ leaving a saddle σ_1 must approach a saddle σ_2. Moreover, this separatrix cannot connect σ_1 to itself, i.e. $\sigma_1 \neq \sigma_2$. In fact, let $\sigma_1 = \sigma_2$, since there holds that $\arg h(z^{\perp}(t)) =$ constant,

$$\lim_{t \downarrow 0} \arg h(z^{\perp}(t)) = \arg h(\sigma_1) \quad \text{and also} \quad \lim_{t \uparrow 0} \arg h(z^{\perp}(t)) = \arg h(\sigma_1),$$

which is impossible, see Fig. 8 and the comments on Fig. 1.

Note that—when introducing rotated Newton flows—no additional restrictions were laid upon the function f. But now, we return to the case of *non-degenerate* functions f. Then $\overline{\overline{\mathcal{N}}}^{\perp}(f)$ has $2r$ simple saddles (corresponding to the critical points for f) with altogether $4r$ separatrices, connecting *different* saddles. So, we may introduce:

Definition 2.18 The graph $\mathcal{G}^{\perp}(f)$, $f \in \check{E}_r$, on the torus T is given by:

- Vertices are the $2r$ critical points for f (as saddles for $\overline{\overline{\mathcal{N}}}^{\perp}(f)$) on T.
- Edges are the $4r$ separatrices at the critical points for f (as $\overline{\overline{\mathcal{N}}}^{\perp}(f)$-saddles) on T.

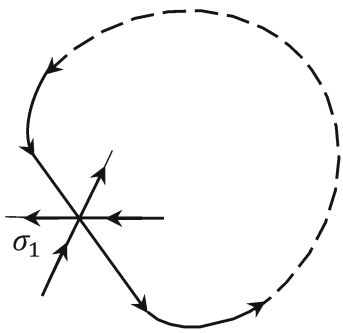

Fig. 8 No "self-connected" $\overline{\overline{\mathcal{N}}}^{\perp}(h)$-saddles; σ_1 is twofold; $h(z) = \exp(-i \log f(z))$

Since all zeros and poles for f are centers for $\overline{\overline{\mathcal{N}}}^{\perp}(f)$, each $\mathcal{G}^{\perp}(f)$-face contains only one zero or one pole for f. Moreover, the graph $\mathcal{G}^{\perp}(f)$ is cellularly embedded. Hence, the graph $\mathcal{G}^{\perp}(f)$ has $2r$ faces.

Lemma 2.19 *Let c be an arbitrary, strictly positive real number and put $L_c = \{z: |f(z)| = c\}$. Then there holds:*

(i) *The level set L_c is a regular curve in $\mathbb{R}^2$ (i.e., $\operatorname{grad} |f(z)| \neq 0$ for all $z \in L_c$) if and only if L_c contains no critical points for f.*
(ii) *The graph $\mathcal{G}^{\perp}(f)$, $f \in \check{E}_r$, is connected. In particular, $f(z)$ admits the same absolute value at all critical points z.*

Proof (i) Use the Cauchy–Riemann equations. (ii) Apply Euler's formula for toroidal graphs (cf. [5]). □

We orient the edges of $\mathcal{G}^{\perp}(f)$ according to their orientation as $\overline{\overline{\mathcal{N}}}^{\perp}(f)$-trajectories. Let A_i and B_j be open subsets of $\mathbb{C}$, corresponding to the (open) faces of $\mathcal{G}^{\perp}(f)$ that are determined by the zero a_i, respectively the pole b_j, for f. Hence, the boundaries of A_i are clockwise oriented, but those of B_j anti-clockwise. Since $\overline{\overline{\mathcal{N}}}^{\perp}(1/f) = -\overline{\overline{\mathcal{N}}}^{\perp}(f)$ we have: reversing the orientations in $\mathcal{G}^{\perp}(f)$ turns this graph into $\mathcal{G}^{\perp}(1/f)$ and thus, by Lemma 2.19 (ii), $|f(z)| = 1$ on $\mathcal{G}^{\perp}(f)$. See Fig. 9 for (parts of) the graphs $\mathcal{G}^{\perp}(f)$, $\mathcal{G}(f)$, $\mathcal{G}^{*}(f)$ and $\mathcal{G}^{\perp}(1/f)$, $\mathcal{G}(1/f)$, $\mathcal{G}^{*}(1/f)$. A canonical $\overline{\overline{\mathcal{N}}}(f)$-region, with $[a_i]$, $[b_j]$ in opposite position, and the saddles σ, σ' consecutive w.r.t. the orientation of A_i (or B_j), will be denoted by $R_{ij}(\sigma, \sigma')$ and it is contained in $F_{a_i}(1/f) \cap F_{b_j}(f)$. Note that, in general, this intersection contains more canonical regions of type $R_{ij}(\cdot, \cdot)$. But even so, these regions are separated by canonical regions, not of this type; compare Remark 2.8. In view of Sect. 1.1 and Lemma 2.17 (i), under f the net of $\overline{\overline{\mathcal{N}}}(f)$- and $\overline{\overline{\mathcal{N}}}(f)^{\perp}$-trajectories on $R_{ij}(\sigma, \sigma')$ is homeomorphically mapped onto a polar net in a sector of the $(u + iv)$-plane ($u = \operatorname{Re} f$, $v = \operatorname{Im} f$), namely

$$s_{ij}(\sigma, \sigma') = \left\{ (u, v): 0 < u^2 + v^2 < \infty,\ \arg f(\sigma) < \arctan \frac{v}{u} < \arg f(\sigma') \right\}.$$

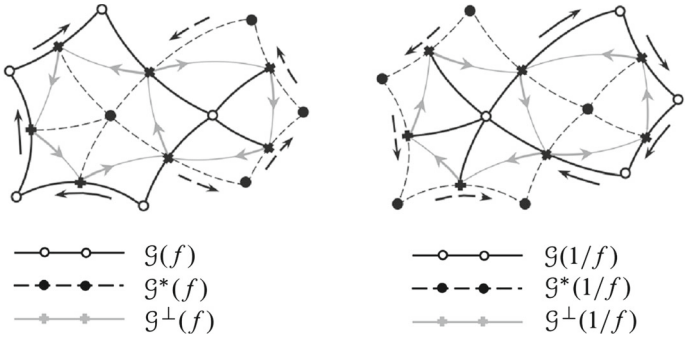

Fig. 9 The graphs $\mathcal{G}(\cdot)$, $\mathcal{G}^*(\cdot)$ and $\mathcal{G}^\perp(\cdot)$ for f and $1/f$ in $\widetilde{E}_r$

Analogously, $1/f$ maps the net of $\overline{\overline{\mathcal{N}}}(f)$- and $\overline{\overline{\mathcal{N}}}(f)^\perp$-trajectories on $R_{ji}(\sigma, \sigma')$ onto a polar net in a sector of the $(U + iV)$-plane ($U = \operatorname{Re} 1/f$, $V = \operatorname{Im} 1/f$), namely

$$S_{ij}(\sigma, \sigma') = \left\{ (U, V) : 0 < U^2 + V^2 < \infty,\ -\arg f(\sigma) < \arctan \frac{V}{U} < -\arg f(\sigma') \right\}.$$

So, the polar nets on $s_{ij}(\sigma, \sigma')$ and $S_{ij}(\sigma, \sigma')$ correspond under the inversion[7]

$$U = \frac{u}{u^2 + v^2}, \qquad V = \frac{v}{u^2 + v^2}.$$

Next we turn to the relationship between Newton flows and steady streams.

Remark 2.20 (*Newton flows as steady streams*) For $f \in \check{E}_r$, we consider the planar *steady stream* [15] with complex potential $w(z) = -\log f(z)$, potential function $\Phi(x, y) = -\log |f(z)|$ and stream function $\psi(x, y) = -\arg f(z)$, where $x = \operatorname{Re} z$, $y = \operatorname{Im} z$. Then the *equipotential lines* are given by $-\log |f(z)| =$ constant, the *stream lines* by $-\arg f(z) =$ constant and the *velocity field* $V(z)$ ($=\operatorname{grad} \Phi$) by the complex conjugate of $w'(z)$, i.e.

$$V(z) = \frac{|w'(z)|^2}{w'(z)} = \frac{-|w'(z)|^2 f(z)}{f'(z)} \ (= |w'(z)|^2 \mathcal{N}(f)).$$

Moreover, the zeros (poles) for f are just the sinks (sources) of strength 1, whereas the critical points for f are the onefold stagnation points of the stream, compare also [8]. So, the "orthogonal net of the stream- and equipotential-lines" of the planar steady stream is a combination of the phase portraits of $\overline{\mathcal{N}}(f)$ and $\overline{\mathcal{N}}^\perp(f)$, see Fig. 10.

Hence we may interpret the pair $(\overline{\overline{\mathcal{N}}}(f), \overline{\overline{\mathcal{N}}}^\perp(f))$ as a toroidal desingularized version of our planar steady stream.

[7] Here we use that in a canonical region the angles at the zero and the pole are equal.

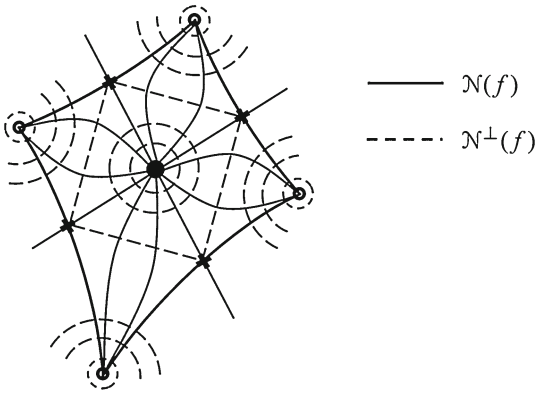

Fig. 10 The steady stream $w(z) = -\log f(z)$, $f \in \check{E}_r$

Finally, we clarify the "steady stream character" of the structurally stable elliptic Newton flows from the point of view of the Riemann surface T.

Firstly, we note that the polar net on open (!) sectors as $s_{ij}(\sigma, \sigma')$ and $S_{ij}(\sigma, \sigma')$ is just the stream and equipotential lines of the steady stream with complex potential $-\log(u+iv)$, respectively $-\log(U+iV)$. In particular, these stream and equipotential lines exhibit the phase portraits of respectively the flows $\mathcal{N}(u+iv)$ $(=-(u+iv))$, $\mathcal{N}(u+iv)^{\perp}$ $(=-i(u+iv))$, and $\mathcal{N}(U+iV)$ $(=-(U+iV))$, $\mathcal{N}(U+iV)^{\perp}$ $(=-i(U+iV))$ on $s_{ij}(\sigma, \sigma')$ and $S_{ij}(\sigma, \sigma')$ respectively. Deleting from T all zeros, poles and critical points for f, we obtain "the reduced torus" $\check{T}$, an open submanifold of T.

Now the collection

$$\left\{ F_{a_i}\left(\frac{1}{f}\right)\backslash[a_i],\, F_{b_j}(f)\backslash[b_j]\colon \;\; i, j = 1, \ldots, r \right\}$$

exhibits a covering of $\check{T}$ with open neighborhoods. Apparently, only in the case of pairs $(F_{a_i}(1/f)\backslash[a_i],\, F_{b_j}(f)\backslash[b_j])$ a non-empty intersection is possible. Even so, the intersection

$$F_{a_i}\left(\frac{1}{f}\right)\backslash[a_i] \cap F_{b_j}(f)\backslash[b_j]$$

consists of the disjoint union of sets of the type $R_{ij}(\cdot, \cdot)$, say $R_{ij}^1, \ldots, R_{ij}^s$. (Note that $[a_i]$ occurs in w_{b_j} as many times as $[b_j]$ occurs in w_{a_i}.) This turns our covering into an atlas for $\check{T}$ with smooth (even complex analytic) coordinate transformations, induced by the inversion $u+iv \leftrightarrow 1/(u+iv) = U+iV$. With aid of this atlas, we may interpret $\overline{\overline{\mathcal{N}}}(f)$ and $\overline{\overline{\mathcal{N}}}^{\perp}(f)$ on each canonical region as the pull back of the most simple[8] planar flows $\mathcal{N}(u+iv)$, $\mathcal{N}^{\perp}(u+iv)$, and $\mathcal{N}(U+iV)$, $\mathcal{N}^{\perp}(U+iV)$ on the various sectors $s_{ij}(\cdot, \cdot)$ and $S_{ij}(\cdot, \cdot)$ respectively. Glueing the canonical regions $R_{ij}(\cdot, \cdot)$ along the

[8] On the sectors $s_{ij}(\sigma, \sigma')$, respectively $S_{ij}(\sigma, \sigma')$, the flows $\mathcal{N}(u+iv)$, respectively $\mathcal{N}(U+iV)$, are parts of North–South flows (cf. [8]).

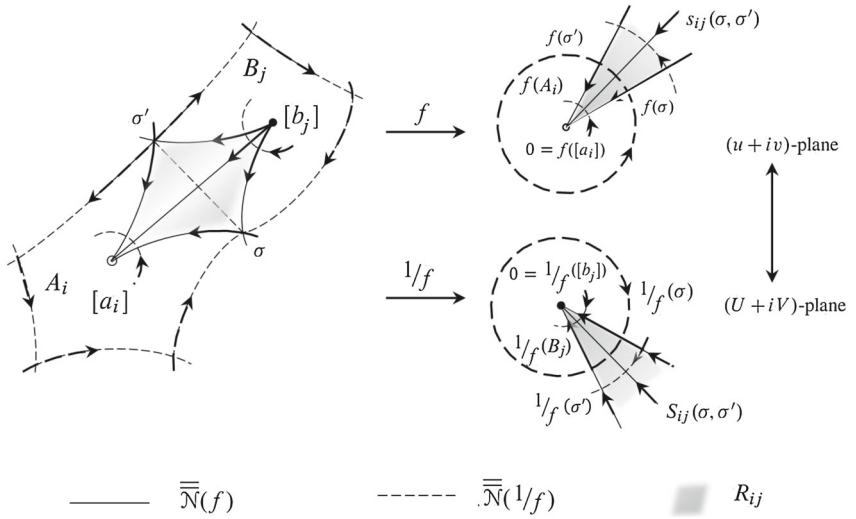

Fig. 11 The canonical regions R_{ij}, and the sectors $s_{ij}(\sigma,\sigma')$ and $S_{ij}(\sigma,\sigma')$

$\overline{\overline{\mathcal{N}}}(f)$-trajectories in their common boundaries, we obtain the restrictions to $\check{T}$ of our original (rotated) Newton flows. In particular, the flows $\mathcal{N}(u+iv)$ $(=-(u+iv))$ and $\mathcal{N}(U+iV)$ $(=-(U+iV))$ lead to an analytic function on $\check{T}$, namely the restriction $f|\check{T}$, with as isolated singularities the zeros, poles and critical points for f. By continuous extension to this singularities, we find the original flows $\overline{\overline{\mathcal{N}}}(f)$ and $\overline{\overline{\mathcal{N}}}^{\perp}(f)$. For an illustration, see Figs. 11 and 12.

3 Newton graphs

Throughout this section, the connected graph $\mathcal{G}$ is a cellular embedding in T, seen as a compact, orientable, Hausdorff topological space of an abstract connected *multigraph* **G** (i.e., no loops) with r vertices, $2r$ edges ($r \geqslant 2$); $r =$ order $\mathcal{G}$.

The forthcoming analysis strongly relies on some concepts from classical graph theory on surfaces, which—in order to fix terminology—will be briefly reviewed.[9]

3.1 Cellularity; geometric duals

Since $\mathcal{G}$ is cellularly embedded, we may consider (cf. [18]) the *rotation system* Π for $\mathcal{G}$:

$$\Pi = \{\pi_v : \text{all vertices } v \text{ in } \mathbf{G}\},$$

[9] Again we follow the treatise [18] closely. Note however, that in [18] a multigraph may exhibit loops, whereas in our case this possibility for $\mathcal{G}$ is ruled out.

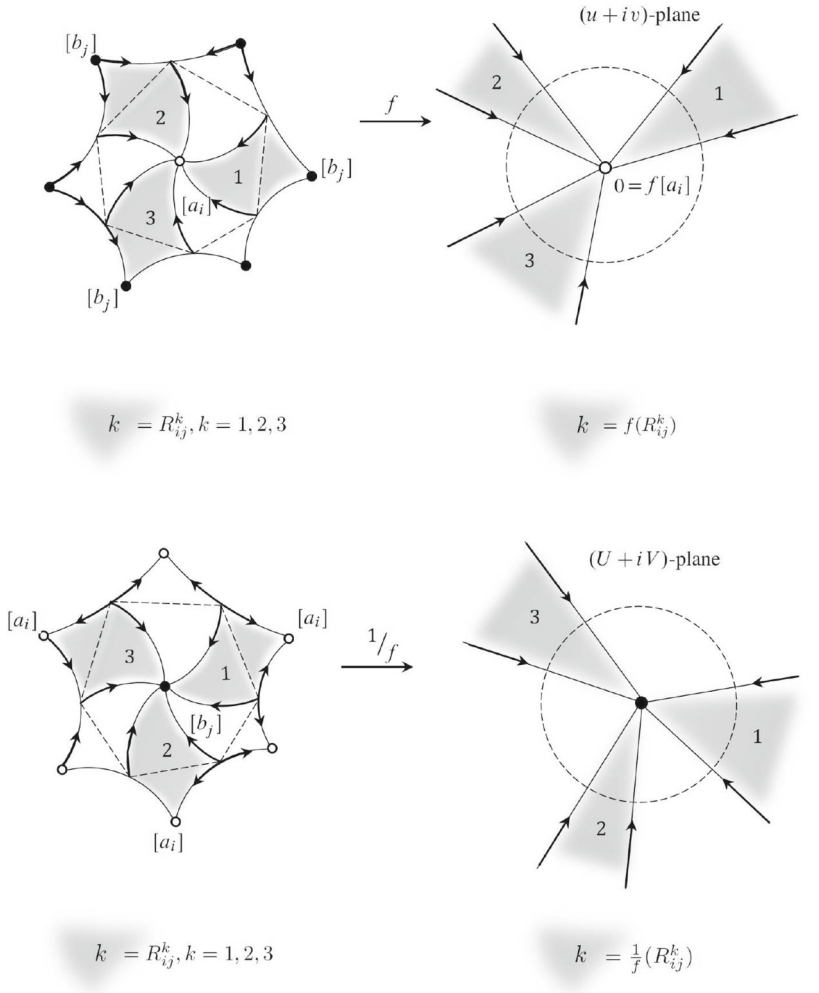

Fig. 12 $F_{a_i}(1/f)\backslash[a_i] \cap F_{b_j}(f)\backslash[b_j]$ and its images under f and $1/f$ $(s = 3)$

where the local *rotation* π_v at v is the cyclic permutation of the edges incident with v such that $\pi_v(e)$ is the successor of e in the anti-clockwise ordering around v.

If $e\ (=v'v'')$ stands for an edge, with end vertices v' and v'', we define a Π-*walk* (facial walk[10]), say w, on $\mathcal{G}$ as follows:

The face traversal procedure: Consider an edge $e_1 = (v_1v_2)$ and the closed walk[11] $w = v_1e_1v_2e_2v_3 \ldots v_ke_kv_1$, which is determined by the requirement that, for $i = 1, \ldots, \ell$, we have $\pi_{v_{i+1}}(e_i) = e_{i+1}$, where $e_{\ell+1} = e_1$ and ℓ is minimal.

[10] Compare the facial walk w_{b_j} in Sect. 2.

[11] We shall not distinguish between w and its cyclic shifts.

Apparently, such "minimal" ℓ exists since $\mathbf{G}$ is finite. Note that each edge occurs *either once* in two different Π-walks, or *twice* (with opposites orientations) in *only one* Π-*walk*; in particular, the first edge in the same direction which is repeated when traversing w, is e_1. As in the proof of Lemma 2.9, these Π-walks can be used to construct (patching the facial polygons along identically labelled sides) a surface S and in S a so-called 24-*cell* embedded graph with faces determined by the facial polygons. By Euler's formula (cf. [5]), there are r facial walks. So, S is homeomorphic to T and the 2-cell embedded graph is isomorphic to $\mathcal{G}$. By the *Heffter–Edmonds–Ringel rotation principle*, the graph $\mathcal{G}$ is uniquely determined up to isomorphism by its rotation system. We say $\mathcal{G}$ is generated by Π.

From now on, we suppress the role of the underlying abstract graph $\mathbf{G}$ and will not distinguish between the vertices of $\mathcal{G}$ and those of $\mathbf{G}$. Occasionally, $\mathcal{G}$ will be referred to as to the pair $(\mathcal{G}, \Pi)$. The $\mathcal{G}$-faces (as well as the corresponding facial polygons) are denoted by F_j; their boundaries (as well as the corresponding Π-walks) by ∂F_j, $j = 1, \ldots, r$. We denote the sets of all vertices, edges and faces of $\mathcal{G}$ by $V(\mathcal{G})$, $E(\mathcal{G})$ and $F(\mathcal{G})$ respectively.

The embedding of $\mathcal{G}$ into the orientable surface T induces an anti-clockwise orientation on the edges around each vertex v. In the sequel we assume that the local rotations π_v are endowed with this orientation (so that the inverse permutations π_v^{-1} are clockwise).

Given a cellularly embedded toroidal $(\mathcal{G}, \Pi)$, the abstract graph $\mathbf{G}^*$ is defined as follows:

- The r vertices $\{v^*\}$ are represented by the Π-walks in $\mathcal{G}$.
- Two vertices are connected by an edge e^* iff the representing Π-walks share an edge e.

Hence, between the $\mathcal{G}$-edges and $\mathbf{G}^*$-edges, there is a bijective correspondence: $e \leftrightarrow e^*$. In particular, $\mathbf{G}^*$ has $2r$ edges, and an edge e^* is a loop[12] iff e shows up twice in a Π-walk of $\mathcal{G}$.

The graph $\mathbf{G}^*$ admits a 2-cell embedding in T: the *(geometric) dual* $(\mathcal{G}^*, \Pi^*)$. In fact, if the vertex v^* in $(\mathcal{G}^*, \Pi^*)$ is represented[13] by the Π-walk $(e_1 - \cdots - e_l)$, then the cyclic permutation on the $\mathbf{G}^*$-edges incident with v^*, say $\pi^*_{v^*}$, is defined by $\pi^*_{v^*} = (e_1^* - \cdots - e_\ell^*)$. A Π^*-walk of length ℓ' corresponds to precisely one $\mathcal{G}$-vertex of degree ℓ': compare Fig. 6, where $\mathcal{G} = \mathcal{G}(f)$ and $\mathcal{G}^* = \mathcal{G}^*(f)$. The anti-clockwise orientation of the local rotation systems in $\mathcal{G}$ induces a clockwise orientation on the Π-walk in $\mathcal{G}$ and thus a clockwise orientation on the rotation systems in $\mathcal{G}^*$. This results—by the face traversal procedure—into an anti-clockwise orientation on the Π^*-walks in $\mathcal{G}^*$.

By $-\mathcal{G}\,(-\mathcal{G}^*)$ we mean $\mathcal{G}$ $(\mathcal{G}^*)$ with the anti-clockwise (clockwise) orientation; compare $-\mathcal{G}(f)$ and $-\mathcal{G}^*(f)$ in Sect. 2. It follows that $(\mathcal{G}^*, \Pi^*)^* = (\mathcal{G}, \Pi)$.

Note that if two cellularly embedded graphs in T are isomorphic, then also their duals are.

[12] In contradistinction to our assumption on $\mathbf{G}$, the graph $\mathbf{G}^*$ may admit loops.

[13] We say: v^* is "located" in the $\mathcal{G}$-face, determined by the Π-walk $(e_1 - \cdots - e_\ell)$.

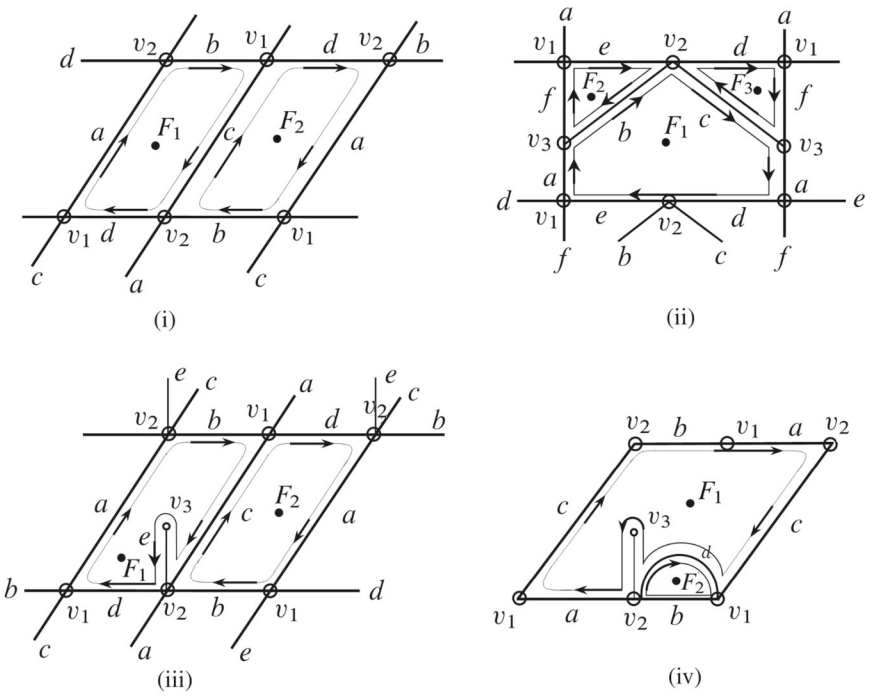

Fig. 13 Four multigraphs, cellularly embedded in T

3.2 The E(Euler)-property

In contradistinction to the case of facial walks in $\mathcal{G}(f)$, $f \in \widetilde{E}_r$, see Lemma 2.7, a Π-walk in $\mathcal{G}$ is in general *not* an Euler-trail. So, we need an additional condition.

Definition 3.1 $(\mathcal{G}, \Pi)$ has the *E(Euler)-property* if every Π-walk is Eulerian.

For an example of a second order graph $(\mathcal{G}, \Pi)$ that has the E-property, see Fig. 13 (i). This is not so for the third order graphs $(\mathcal{G}, \Pi)$ in Fig. 13 (ii), (iii), whereas the graph in Fig. 13 (iv) does not even fulfil the initial conditions laid upon $\mathcal{G}$ (because there are three vertices and only five edges). Note, however, that also in the latter case the Euler characteristic vanishes, so that this multigraph is toroidal as well.

Lemma 3.2 *If* $(\mathcal{G}, \Pi)$ *has the E-property, then this is also true for* $(\mathcal{G}^*, \Pi^*)$.

Proof Recall that the conditions "E-property holds for $\mathcal{G}$" and "non-occurrence of loops in $\mathcal{G}^*$" are equivalent and apply $(\mathcal{G}^*)^* = \mathcal{G}$. □

From now on, we assume that both $\mathcal{G}$ and $\mathcal{G}^*$ are multigraphs and fulfil the E-property. In particular, each edge in these graphs is adjacent to *two different* faces.

Let v be an arbitrary vertex in $\mathcal{G}$, contained in the boundary ∂F of a face F and $e_1 v e_2$ be a subwalk of the Π-walk w_F. The *different* edges e_1, e_2 are consecutive w.r.t. the (*clockwise*) orientation of w_F. The *facial local sector* of F at v, spanned by the

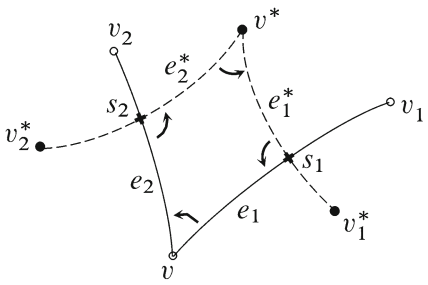

Fig. 14 Pairs of facial sectors in opposite position

ordered pair (e_1, e_2), is referred to as to an *F-sector at* v. Note that if v occurs more than once in w_F, two F-sectors at v cannot share an edge (because in that case the common edge would show up twice in w_F). Hence, F-sectors at v must be separated by facial sectors at v that do not belong to F. So, if $e_1 v e_2$ and $e_1' v e_2'$ are subwalks of w_F, spanning two facial F-sectors at v, then e_1, e_2, e_1' and e_2' must be different. Thus each vertex in ∂F has even degree.

Apparently, the number of all facial sectors at v equals the degree of v, and in $\mathcal{G}$ there are altogether $\delta_1 + \cdots + \delta_r$ $(=4r)$ facial sectors, where the δ_i's stand for the degrees of the vertices in $\mathcal{G}$.

Similarly, there are $\delta_1^* + \cdots + \delta_r^*$ $(=4r)$ facial sectors in $\mathcal{G}^*$ with the δ_j^*'s the degrees of the $\mathcal{G}^*$-vertices.

We write $F = F_{v^*}$, where v^* is the $\mathcal{G}^*$-vertex defined by F. So, $w_F = w_{F_{v^*}}$. Analogously, F_v^* stands for the $\mathcal{G}^*$-face determined by v. Then $e_2^* v^* e_1^*$ is a subwalk of $w_{F_v^*}$ and the *different* edges e_1^*, e_2^* are consecutive w.r.t. the *anti-clockwise* orientation of this facial walk. We say that the F_{v^*}-sector at v, spanned by the pair (e_1, e_2) and the F_v^*-sector at v^* spanned by (e_1^*, e_2^*) are in *opposite position*; see Fig. 14. Altogether there are $4r$ of such (ordered) pairs of $\mathcal{G}$-, $\mathcal{G}^*$-vertices. Note that if v occurs p times in $w_{F_{v^*}}$, then v^* shows up also p times in $w_{F_v^*}$.

The next step is to introduce the analogon of the *common refinement* $\mathcal{G}(f) \wedge \mathcal{G}^*(f)$.

Definition 3.3 The abstract graph $\mathbb{P}(\mathcal{G})$ is given as follows:

- There are $4r$ vertices (on three levels) represented by:
  - the $\mathcal{G}$-vertices [Level-1],
  - the pairs $s = (e, e^*)$, $e \in E(\mathcal{G})$, $e^* \in E(\mathcal{G}^*)$ [Level-2],
  - the $\mathcal{G}^*$-vertices [Level-3].
- There are $8r$ edges:
  - a vertex on Level-2, represented by (e, e^*), is connected to two different vertices on Level-1, namely the $\mathcal{G}$-vertices incident with e, and to two different vertices on Level-3, namely the $\mathcal{G}^*$-vertices incident with e^*,
  - vertices on Level-1 are not connected with vertices on Level-3.

$\mathbb{P}(\mathcal{G})$-vertices on the Levels-1,3 are denoted as the corresponding $\mathcal{G}$-, $\mathcal{G}^*$-vertices. The graph $\mathbb{P}(\mathcal{G})$ is directed by the convention: vertices on Level-1 (respectively Level-3) are the end- (respectively begin-) points of its edges.

We claim the existence of a cellular embedding of $\mathbb{P}(\mathcal{G})$ in T, denoted $\mathcal{G} \wedge \mathcal{G}^*$, with faces determined by the $4r$ pairs of facial sectors in *opposite position*. In order to

verify this claim, consider an arbitrary pair of such sectors, given by the subwalks $e_1 v e_2$ and $e_1^* v^* e_2^*$ with $s_\ell = (e_\ell, e_\ell^*)$, $\ell = 1, 2$; compare Fig. 14. We specify local rotation systems on $\mathbb{P}(\mathcal{G})$ at v and v^* by π_v and $\pi_{v^*}^*$ respectively. The rotation systems at s_1 and s_2 are given by the cyclic permutations $(s_1 v, s_1 v_1^*, s_1 v_1, s_1 v^*)$, respectively $(s_2 v, s_2 v^*, s_2 v_2, s_2 v_2^*)$, where v_ℓ and v_ℓ^* stand for the vertices incident with e_ℓ and e_ℓ^* that are different from respectively v and v^*, $\ell = 1, 2$. The resulting rotation system for $\mathbb{P}(\mathcal{G})$ is called (Π, Π^*). Now starting from $v s_2$ we find the (Π, Π^*)-walk $(v s_2, s_2 v^*, v^* s_1, s_1 v)$.

This yields a cellular embedding of $(\mathbb{P}(\mathcal{G}), (\Pi, \Pi^*))$ into a surface homeomorphic to T (because the alternating sum of the numbers of vertices, edges and (Π, Π^*)-walks in $\mathbb{P}(\mathcal{G})$ vanishes). This embedding is denoted by $\mathcal{G} \wedge \mathcal{G}^*$, and can be viewed as the common refinement of $\mathcal{G}$ and $\mathcal{G}^*$. Each face in $\mathcal{G} \wedge \mathcal{G}^*$ is represented by a quadruple of directed edges in $\mathbb{P}(\mathcal{G})$ and is associated with exactly one vertex on Level-1, one vertex on Level-3 (in opposite position) and two vertices on Level-2. Moreover, each $\mathcal{G}$-face ($\mathcal{G}^*$-face) is built up from the sets of all $\mathcal{G} \wedge \mathcal{G}^*$-faces centered at a $\mathcal{G}^*$-vertex ($\mathcal{G}$-vertex), ordered in accordance with the orientation of $\mathcal{G}$ ($\mathcal{G}^*$). This observation turns the *abstract* graph $\mathbb{P}(\mathcal{G})$ into a distinguished graph $\mathbb{P}^{\mathrm{d}}(\mathcal{G})$ with only distinguished sets of Type 1 (in the sense of [20]).

Following Peixoto, the distinguished graph $\mathbb{P}^{\mathrm{d}}(\mathcal{G})$ is realizable as *the* distinguished graph of a C^1-*structurally stable* vector field, say[14] $\mathcal{X}(\mathcal{G})$ on T, with

- as hyperbolic attractors (repellors): the $\mathcal{G}$-vertices ($\mathcal{G}^*$-vertices),
- as onefold saddles: the other $\mathcal{G} \wedge \mathcal{G}^*$-vertices,
- as stable (unstable) separatrices at the saddles: the $\mathcal{G} \wedge \mathcal{G}^*$-edges with as begin point a $\mathcal{G}^*$-vertex (as end point a $\mathcal{G}$-vertex),
- as canonical regions (of Type 1): the faces of $\mathcal{G} \wedge \mathcal{G}^*$.

Note that $\mathcal{X}(\mathcal{G})$ exhibits *no* "saddle connections", *no* closed orbits and thus *no* limit cycles.

In order to specify the roles of $\mathcal{G}$ and $\mathcal{G}^*$, we occasionally write $\mathcal{X}(\mathcal{G}) = \mathcal{X}_{\mathcal{G} \wedge \mathcal{G}^*}$.

Again, due to Peixoto's classification result [20] on structural stability, we have[15]: If $\mathcal{H}$ is any connected multigraph such as $\mathcal{G}$ (i.e., cellularly embedded in T, the E-property holds, all Π-walks are clockwise oriented, r vertices, $2r$ edges) then

$$\mathcal{X}_{\mathcal{G} \wedge \mathcal{G}^*} \sim \mathcal{X}_{\mathcal{H} \wedge \mathcal{H}^*} \iff \mathcal{G} \sim \mathcal{H} \ \text{ (and thus } \mathcal{G}^* \sim \mathcal{H}^*),$$

where, as in Sect. 2, in the l.h.s. $\sim$ stands for conjugacy and in the r.h.s. for equivalency, an isomorphism between graphs respecting their orientations.[16]

The flow $\mathcal{X}(\mathcal{G}^*)$ is the *dual version* of $\mathcal{X}(\mathcal{G})$, i.e., $\mathcal{X}(\mathcal{G}^*)$ is obtained from $\mathcal{X}(\mathcal{G})$ by reversing the orientations of the trajectories of the latter flow, thereby changing

[14] Since $\mathcal{G}^*$ is determined by $\mathcal{G}$, we occasionally refer to $\mathcal{G}$ as to the distinguished graph of $\mathcal{X}(\mathcal{G})$.

[15] In fact, $\mathcal{X}_{\mathcal{G} \wedge \mathcal{G}^*} \sim \mathcal{X}_{\mathcal{H} \wedge \mathcal{H}^*} \Leftrightarrow \mathbb{P}^{\mathrm{d}}(\mathcal{G}) \sim \mathbb{P}^{\mathrm{d}}(\mathcal{H})$, where $\sim$ is defined as in (4).

[16] More precisely, if Π and Π' are rotation systems for $\mathcal{G}$ respectively $\mathcal{H}$, then either $\pi'_{\varphi(v)} = \pi_v$ for all $v \in V(\mathcal{G})$, or $\pi'_{\varphi(v)} = \pi_v^{-1}$ for all $v \in V(\mathcal{G})$, where φ is a homeomorphism on T with $\varphi(\mathcal{G}) = \mathcal{H}$. In the first case we call φ orientation-preserving and in the second case orientation-reversing.

repellors into attractors and vice versa. Since $(\mathcal{G}^*)^* = \mathcal{G}$, the dual version of $\mathcal{X}(\mathcal{G}^*)$ is $\mathcal{X}(\mathcal{G})$.

Now, put $\mathcal{H} = -\mathcal{G}^*$, then

$$\mathcal{X}(\mathcal{G}) \sim \mathcal{X}(-\mathcal{G}^*) \iff \mathcal{G} \sim -\mathcal{G}^*. \qquad [\textit{self-duality}]$$

This observation can be paraphrased as:

Lemma 3.4 *$\mathcal{X}(\mathcal{G})$ is self-dual iff $\mathcal{G}$ is self-dual.*

Put $\delta(\mathcal{G}) = \{\delta_i = \deg(v_i) : v_i \in V(\mathcal{G})\}$ and $\delta^*(\mathcal{G}) = \{\delta_j^* = \deg(v_j^*) : v_j^* \in V(\mathcal{G}^*)\}$, then:

Lemma 3.5 $\mathcal{G} \sim -\mathcal{G}^* \Leftrightarrow \delta(\mathcal{G}) = \delta^*(\mathcal{G})\ (=\delta(\mathcal{G}^*))$.

Proof Note that the δ_i's together with the claim "clockwise" ("anti-clockwise") fix the local rotations of $\mathcal{G}$ and $\mathcal{G}^*$. Now the Heffter–Edmonds–Ringel rotation principle together with $(\mathcal{G}^*)^* = \mathcal{G}$ proves the assertion. □

From Lemmata 3.4 and 3.5 it follows:

Corollary 3.6 $\mathcal{X}(\mathcal{G}) \sim \mathcal{X}(-\mathcal{G}^*) \Leftrightarrow \delta(\mathcal{G}) = \delta^*(\mathcal{G})$.

3.3 The A(Angle)-property

Recall that $V(\mathcal{G}) = \{v_1, \ldots, v_r\}$ and $\delta_i = \deg(v_i)$. The δ_i anti-clockwise ordered edges, incident with the vertex v_i, are denoted $e_{i(k)}, e_{i(\delta_i+1)} = e_{i(1)}$, $k = 1, \ldots, \delta_i$. Note that all these edges are different (because $\mathcal{G}$ is a multigraph). Since T is locally homeomorphic to an open disk, it is always possible to re-draw $\mathcal{G}$, thereby respecting Π such that the anti-clockwise measured angles at v_i between $e_{i(k)}$ and $e_{i(k+1)}$, say $2\pi\,\omega_{i(k)}$, are strictly positive and sum up to 2π. The resulting graph is again denoted by $\mathcal{G}$. Since $\mathcal{G}$ is a multigraph, we have altogether $4r$ $(=\delta_1 + \cdots + \delta_r)$ "angles" $\omega_{i(k)}$. The set of all these angles is $A(\mathcal{G})$. The subset of all angles between edges that are consecutive edges in the Π-walk w_{F_j} that span an F_j-sector, is called the set of angles of F_j and will be denoted by $a(F_j)$. Finally, for fixed i, the set of all "angles" $\omega_{i(k)}$, $k = 1, \ldots, \delta_i$, is the "set $a(v_i)$ of angles at v_i".

Definition 3.7 $\mathcal{G}$ has the *A(Angle)-property* if, possibly under a suitable local re-drawing, the angles in $A(\mathcal{G})$ can be chosen such that:

(A_1) $\omega_{i(k)} > 0$ for all $\omega_{i(k)} \in A(\mathcal{G})$.
(A_2) $\sum_{a(v_i)} \omega_{i(k)} = 1$ for all $i = 1, \ldots, r$.
(A_3) $\sum_{a(F_j)} \omega_{i(k)} = 1$ for all $j = 1, \ldots, r$.

Note that conditions (A_1) and (A_2) can always be fulfilled; the crucial claim is condition (A_3).

Moreover, the sets of angles at the vertices v of $\mathcal{G}$ that fulfil conditions (A_1) and (A_2) fix the anti-clockwise oriented local rotations π_v. Hence, $\mathcal{G}$ is determined by these angles.

Let J be an arbitrary *non-empty* subset of $\{1,\dots,r\}$. The subgraph of $\mathcal{G}$ generated by all vertices and edges in the faces F_j, $j\in J$, is denoted by $\mathcal{G}(J)$. An *interior vertex* of $\mathcal{G}(J)$ is a vertex of $\mathcal{G}$ that is only incident with $\mathcal{G}$-faces labelled by J, whereas a vertex of $\mathcal{G}(J)$ is called *exterior* if it is incident with both a face labelled by J and a face *not* labelled by J. The sets of all interior, respectively all exterior, vertices in $\mathcal{G}(J)$ are denoted by $\operatorname{Int}\mathcal{G}(J)$ and $\operatorname{Ext}\mathcal{G}(J)$ respectively. If $J=\{1,\dots,r\}$, then $|\operatorname{Int}\mathcal{G}(J)|=|J|=|V(\mathcal{G}(J))|=|V(\mathcal{G})|\ (=r)$, where as usual $|\cdot|$ stands for cardinality.

Lemma 3.8 *Assume that $\mathcal{G}$ fulfils the A-property. Then*

$$|\operatorname{Int}\mathcal{G}(J)|<|J|<|V(\mathcal{G}(J))| \quad \textit{for all } J,\ \varnothing\neq J\subsetneq\{1,\dots,r\}. \tag{5}$$

Proof By Definition 3.7,

$$\sum_{j\in J}\sum_{a(F_j)}\omega_{i(k)}=|J|.$$

The contribution of any *interior* vertex of $\mathcal{G}(J)$ to the sum in the l.h.s. of this equation is equal to 1, whereas each *exterior* vertex contributes with a number that is strictly between 0 and 1. Hence, we are done if—for the subsets J under consideration—we can prove that $\operatorname{Ext}\mathcal{G}(J)\neq\varnothing$. So, assume $\operatorname{Ext}\mathcal{G}(J)$ is empty, thus $\operatorname{Int}\mathcal{G}(J)\neq\varnothing$. Let J^{C} be the complement of J in $\{1,\dots,r\}$. Thus $\varnothing\neq J^{\mathrm{C}}\subsetneq\{1,\dots,r\}$ and $\operatorname{Ext}\mathcal{G}(J^{\mathrm{C}})$ $(=\operatorname{Ext}\mathcal{G}(J))=\varnothing$. Hence, we also have $\operatorname{Int}\mathcal{G}(J^{\mathrm{C}})\neq\varnothing$. Now, the connectedness of $\mathcal{G}$ yields a contradiction. □

Remark 3.9 If $\mathcal{G}$ has the A-property, then: l.h.s. of (5) $\Leftrightarrow$ r.h.s. of (5), so that one of these equalities is redundant.

Lemma 3.10 *If $\mathcal{G}$ fulfils $|J|<|V(\mathcal{G}(J))|$ for all J, $\varnothing\neq J\subsetneq\{1,\dots,r\}$ (cf. (5)), then:*

Any assignment of an arbitrary vertex v_{i_0} to any face F_{j_0} adjacent to v_{i_0}, can be extended to a bijection $\mathcal{T}\colon V(\mathcal{G})\to F(\mathcal{G})$, with $v\in V(\partial\mathcal{T}(v))$ and $\mathcal{T}(v_{i_0})=F_{j_0}$, i.e., the assignment $v_{i_0}\mapsto F_{j_0}$ can be extended to a transversal of the vertex sets $V(\partial F_j)$, $j=1,\dots,r$. (6)

Proof Consider the vertex set $V(\partial F_j)$ of ∂F_j. Put for $j\in\{1,\dots,r\}$, $p_j=1$, if $j\neq j_0$, and $p_{j_0}=0$. For *all non-empty* subsets J of $\{1,\dots,r\}$ (i.e. including $J=\{1,\dots,r\}$), we have

$$|V(\mathcal{G}(J))\backslash\{v_{i_0}\}|\geqslant\sum_{j\in J}p_j.$$

According to a slight generalization of Hall's theorem on distinct representatives (cf. [17]), these inequalities are necessary and sufficient for the existence of pairwise disjoint sets $X_1,\dots,X_r$, such that

$$X_j\subset V(\partial F_j)\backslash\{v_{i_0}\}\qquad\text{with }\ |X_j|=p_j,\quad j=1,\dots,r.$$

Hence, the singletons (!) X_j, $j \in \{1, \ldots, r\}$, $j \neq j_0$, together with v_{i_0} yield the existence of the desired transversal $\mathcal{T}$. □

Now, let us re-label the angles of $\mathcal{G}$ by x_λ, with $\lambda = 1, \ldots, 4r (= \sum_{i=1}^{r} \deg(v_i))$. We associate with $\mathcal{G}$ a $2r \times 4r$-matrix $M(\mathcal{G})$ with coefficients $m_{\ell\lambda}$:

$$m_{\ell\lambda} = \begin{cases} 1, & \text{if } \ell = 1, \ldots, r, \text{ and } x_\lambda \text{ is an angle at } v_\ell, \text{ i.e. } x_\lambda \text{ in } a(v_\ell); \\ 1, & \text{if } \ell = r+1, \ldots, 2r, \text{ and } x_\lambda \text{ is an angle in } a(F_{\ell-r}); \\ 0, & \text{otherwise.} \end{cases}$$

Apparently, $\mathcal{G}$ has the A-property if and only if the following system of $2r$ equations and $4r$ inequalities has a solution:

$$\begin{cases} [M(\mathcal{G}) \mid -1] \cdot (x \mid 1)^{\mathrm{T}} = (0, \ldots, 0)^{\mathrm{T}}, \\ x_\lambda > 0, \quad \lambda = 1, \ldots, 4r. \end{cases} \tag{7}$$

Here, $[M(\mathcal{G}) \mid -1]$ stands for the matrix $M(\mathcal{G})$ augmented with a $(4r+1)$-st column, each of its elements being equal to -1, and $(x \mid 1) = (x_1, \ldots, x_{4r}, 1)$.

Basically due to Stiemke's theorem (cf. [14]), system (7) has a solution *iff* system (8) below has no solution for which at least one of the inequalities is strict:

$$\left(\frac{M(\mathcal{G})^{\mathrm{T}}}{-1 \cdots -1}\right) . Z^{\mathrm{T}} \geqslant (0, \cdots, 0)^{\mathrm{T}}, \tag{8}$$

with $Z = (z_1, \ldots, z_i, \ldots, z_r, \ldots, z_{r+j}, \ldots, z_{2r})$. Here,

$$\left(\frac{M(\mathcal{G})^{\mathrm{T}}}{-1 \cdots -1}\right)$$

stands for the matrix $M(\mathcal{G})^{\mathrm{T}}$ augmented with a $(4r+1)$-st row, all its coefficients being equal to -1. For $i, j \in \{1, \ldots, r\}$, the pair (i, j) is called *associated*, notation $(i, j) \in \mathbf{O}$, if v_i and F_j share an angle.

Obviously, system (8) is equivalent with

$$\begin{cases} z_i + z_{r+j} \geqslant 0, & \text{for all } (i, j) \in \mathbf{O}, \\ \sum_{\ell=1}^{2r} z_\ell \leqslant 0. \end{cases} \tag{9}$$

But now we are in the position to apply Lemma 3.10.

Lemma 3.11 *Consider a graph $\mathcal{G}$, not necessarily with the E-property. Then we have*

$$\mathcal{G} \text{ has the A-property} \Leftrightarrow |J| < |V(\mathcal{G}(J))| \text{ for all } J, \varnothing \neq J \subsetneq \{1, \ldots, r\}.$$

Proof ($\Rightarrow$). See Lemma 3.8.

($\Leftarrow$). Suppose that $Z = (z_1, \ldots, z_{2r})$ is a solution of system (9) for which at least one of the inequalities is not strict. We lead this assumption to a contradiction.

Consider an associated pair (i_0, j_0). So, the vertex v_{i_0} and the face F_{j_0} have an angle in common. Extend by Lemma 3.10, the assignment $v_{i_0} \mapsto F_{j_0}$ to a transversal $\mathcal{T}$ as in (6) and define $\tau(i)$ by $F_{\tau(i)} = \mathcal{T}(v_i)$. This means that v_i and $F_{\tau(i)}$ share an angle, thus $(i, \tau(i)) \in \mathbf{O}$; in particular, $(i_0, \tau(i_0)) = (i_0, j_0) \in \mathbf{O}$. Since Z fulfills (9), we have $z_i + z_{r+\tau(i)} \geqslant 0$, $i = 1, \ldots, r$, and moreover (use that $\mathcal{T}$ is bijective) also

$$\sum_{i=1}^{r}(z_i + z_{r+\tau(i)}) = \sum_{\ell=1}^{2r} z_\ell \leqslant 0.$$

Hence, $z_i + z_{r+\tau(i)} = 0$, $i = 1, \ldots, r$. In particular, $z_{i_0} + z_{r+j_0} = 0$. Since the associated pair (i_0, j_0) was chosen arbitrarily, we have $z_i + z_{r+j} = 0$, for every combination $(i, j) \in \mathbf{O}$. This contradicts our assumption on Z. It follows that system (9) *does not have* a solution for which at least one of the inequalities is strict. Thus system (7) *does admit* a solution, i.e. $(\mathcal{G}, \Pi)$ has the A-property. □

Corollary 3.12 *Let $\mathcal{G}$ be a graph as in Lemma 3.11. Then there holds:*

$$\mathcal{G} \textit{ has the A-property } \Leftrightarrow \textit{ condition (6) holds for } \mathcal{G}.$$

Proof ($\Rightarrow$). See Lemmata 3.8, 3.10. ($\Leftarrow$). Follows from the ($\Leftarrow$) part of the proof of Lemma 3.11. □

The (equivalent) conditions "$|J| < |V(\mathcal{G}(J))|$ for all J, $\varnothing \neq J \subsetneq \{1, \ldots, r\}$" and (6) will be referred to as to the *H(Hall)-condition*; see also Sect. 5.2.

As it can be easily verified, the graphs $\mathcal{G}$ in Fig. 13 (i), (ii) fulfil the *H-condition*, but $\mathcal{G}$ in Fig. 13 (iii) does not. Hence, by Lemma 3.11, or Corollary 3.12, the graphs $\mathcal{G}$ in Fig. 13 (i), (ii) have the A-property, but this is not so for the graph in Fig. 13 (iii).

3.4 Newton graphs

Definition 3.13 Cellularly embedded toroidal graphs with r vertices, $2r$ edges (and thus r faces) that fulfil the A- and E-properties are called *Newton graphs of rank r*.

Lemma 3.14 *If $(\mathcal{G}, \Pi)$ is a Newton graph, then this is also true for $(\mathcal{G}^*, \Pi^*)$.*

Proof In view of Lemma 3.2, we only have to show that $(\mathcal{G}^*, \Pi^*)$ has the A-property. Let v_0^* be a $\mathcal{G}^*$-vertex and consider an assignment $v_0^* \mapsto F_{v_0}^*$, where $F_{v_0}^*$ is a $\mathcal{G}^*$-face adjacent to v_0^* corresponding with the $\mathcal{G}$-vertex v_0. So the pair (v_0, v_0^*) is in opposite position, and v_0 is adjacent to the $\mathcal{G}^*$-face $F_{v_0^*}$. By assumption, $\mathcal{G}$ fulfills the A-property. So, we can extend (by Corollary 3.12) the assignment $v_0 \mapsto F_{v_0^*}$ to a transversal of the vertex sets of $\mathcal{G}$ (i.e., to pairs (v_i, v_i^*) in opposite position such that all v_i and v_i^* are different), and thus to a transversal $v_i^* \to F_{v_i}^*$ of the vertex sets of $\mathcal{G}^*$-faces (extending $v_0^* \mapsto F_{v_0^*}$). Now, application of Corollary 3.12 yields the assertion. □

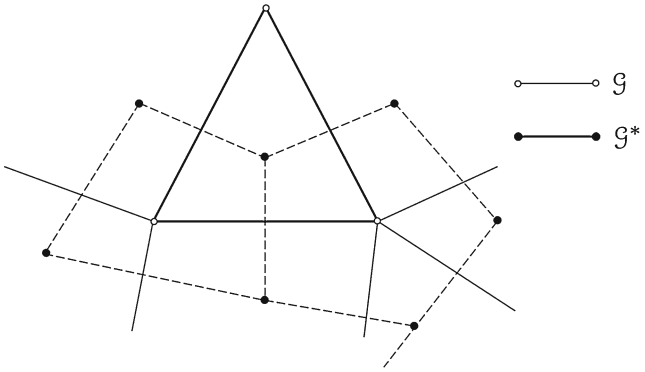

Fig. 15 $(\mathcal{G}, \Pi)$ and its dual $(\mathcal{G}^*, \Pi^*)$; partial

The above result is easily verified by a geometric argument. Consider (under the assumption that the A- and E-properties hold for $\mathcal{G}$) the graph $\mathcal{G} \wedge \mathcal{G}^*$ on T and proceed in two steps (see Fig. 15):

Step 1: Re-draw $\mathcal{G} \wedge \mathcal{G}^*$ locally around the vertices of $\mathcal{G}$ (solid lines) such that the angles in $A(\mathcal{G})$ fulfil conditions (A_1)–(A_3) (in Definition 3.7).

Step 2: Due to condition (A_3) for $\mathcal{G}$, we may re-draw $\mathcal{G} \wedge \mathcal{G}^*$ locally around the vertices of $\mathcal{G}^*$ (dotted lines) such that the $A(\mathcal{G})$- and $A(\mathcal{G}^*)$-angles of facial sectors in opposite position are equal.

We conclude that also $\mathcal{G}^*$ has the A-property, and find as a by-product:

Lemma 3.15 *If $\mathcal{G}$ is a Newton graph, we may assume* (*possibly after a suitable local re-drawing*) *that in each face of $\mathcal{G} \wedge \mathcal{G}^*$ the angles at the $\mathcal{G}$- and $\mathcal{G}^*$-vertices are equal* (*and non-vanishing*).

From now on we assume that a Newton graph and its dual are always oriented as $\mathcal{G}$ and $\mathcal{G}^*$ in Sect. 3.1. From Corollary 2.6 and Lemma 2.7 it follows:

Corollary 3.16 *$\mathcal{G}(f)$ and $\mathcal{G}^*(f)$, $f \in \widetilde{E}_r$, are Newton graphs.*

In the forthcoming section we prove that in a certain sense the reverse is also true. We end up this section with a lemma that we will use in the sequel:

Lemma 3.17 *Let $\mathcal{G}$ be of order $r = 2$ or 3. Then, if $r = 2$, the A-property always holds, whereas in case $r = 3$ the E-property implies the A-property.*

Proof Let J be an arbitrary *non-empty, proper* subset of $\{1, \ldots, r\}$.

Case $r = 2$: Note that $|J| = 1$, thus $|V(\mathcal{G}(J))| > 1$ (because $\mathcal{G}$ has no loops). So we have $|V(\mathcal{G}(J))| > |J|$, i.e., the H-condition holds, and Lemma 3.11 yields the assertion.

Case $r = 3$: If $|J| = 1$, then $|V(\mathcal{G}(J))| > 1$ (because $\mathcal{G}$ has no loops), thus $|V(\mathcal{G}(J))| > |J|$. If $|J| = 2$, then $|J^c| = 1$ and $|V(\mathcal{G}(J^c))| \geqslant 2$ (since $\mathcal{G}$ has no

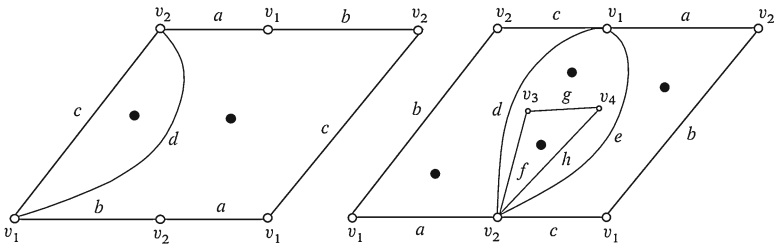

Fig. 16 Two graphs $\mathcal{G}$

loops). Moreover, by the E-property, each edge must be adjacent to at least two faces. This implies that $\text{Int}\,\mathcal{G}(J^c) = \varnothing$. Thus $|\text{Ext}\,\mathcal{G}(J)| = |\text{Ext}\,\mathcal{G}(J^c)| = |V(\mathcal{G}(J^c))| \geqslant 2$ and $|V(\mathcal{G}(J))| = |\text{Ext}\,\mathcal{G}(J)| + |\text{Int}\,\mathcal{G}(J)|$. Distinguish now between two cases:

- $\text{Int}\,\mathcal{G}(J) \neq \varnothing$, then $|V(\mathcal{G}(J))| > |J|$.
- $\text{Int}\,\mathcal{G}(J) = \varnothing$, then the *three* vertices of $\mathcal{G}$ must be exterior vertices for $\mathcal{G}(J)$, thus also $|V(\mathcal{G}(J))| > |J|$. Hence, $|V(\mathcal{G}(J))| > |J|$ holds for all J under consideration, and Lemma 3.11 yields the assertion. □

Remark 3.18 In contradistinction to the A-property, the E-property does not hold for all second order multigraphs $\mathcal{G}$; compare Fig. 16 (i), where the dual $\mathcal{G}^*$ admits a loop. From Fig. 16 (ii), it follows that Lemma 3.17 ($r = 3$) is not true in the case that $r = 4$. From Fig. 13 (ii) we learn that the A-property does not imply the E-property, even if $r = 3$.

4 Structurally stable elliptic Newton flows: representation

In this section we prove that the reverse of Corollary 3.16 is also true.

Theorem 4.1 *Any Newton graph $\mathcal{G}$ of order r can be realized* (*up to equivalency*) *as the graph $\mathcal{G}(f)$, $f \in \widetilde{E}_r$.*

The proof is based on several steps. Starting point is an arbitrary Newton graph $\mathcal{G}$. We apply the results of Sect. 3. Let $\mathcal{X}(\mathcal{G})$ be a C^1-structurally stable vector field on T without limit cycles, determined (up to conjugacy) by $\mathcal{G} \wedge \mathcal{G}^*$, thus by $\mathcal{G}$ as the "distinguished graph" of $\mathcal{X}(\mathcal{G})$ (cf. Footnote 14).

The flow $\mathcal{X}(\mathcal{G})$ is gradient like, i.e. up to conjugacy equal to a gradient flow (with respect to a C^1-Riemannian metric R on T). This can be seen as follows: an arbitrary equilibrium, say $\mathbf{x}$, of the (structurally stable!) flow $\mathcal{X}(\mathcal{G})$ is of hyperbolic type, i.e. the derivative $D_{\mathbf{x}}\mathcal{X}(\mathcal{G})$ has eigenvalues $\lambda_1(\mathbf{x}), \lambda_2(\mathbf{x})$ with non-vanishing real parts, cf. [19]. By the Theorem of Grobman–Hartman [7] (use also [13, Theorem 8.1.8, Remark 8.1.10]), on a suitable $\mathbf{y}$-coordinate neighborhood [with $\mathbf{y} = (y_1, y_2)^{\mathrm{T}}$] of $\mathbf{x}$, the phase portrait of $\mathcal{X}(\mathcal{G})$ is conjugate with the phase portrait around $\mathbf{y} = \mathbf{0}$ of one of the flows given by

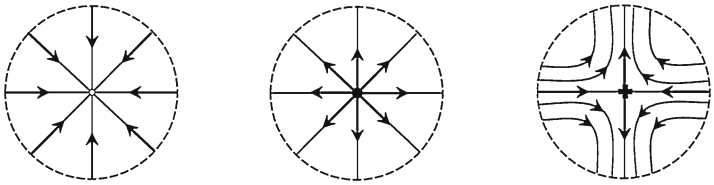

Fig. 17 The possible local phase portraits of $\mathcal{X}(\mathcal{G})$ around $\mathbf{y} = \mathbf{0}$

$$\mathbf{y}' = -\begin{pmatrix} \lambda_1 & 0 \\ 0 & \lambda_2 \end{pmatrix}\mathbf{y}, \quad \mathbf{y}(\mathbf{0}) = \mathbf{0}, \qquad \text{with either } \lambda_1 = \lambda_2 = 1, \text{ or } \lambda_1 = \lambda_2 = -1 \text{ or } \lambda_1 = -\lambda_2 = 1,$$

corresponding to the cases where $\mathbf{y} = \mathbf{0}$ stands for respectively a *stable star node*, an *unstable star node* and an *orthogonal saddle*; see comments on Figs. 1 and 17.

Applying a flow box argument ("cutting" and "pasting" of local phase portraits), we find that $\mathcal{X}(\mathcal{G})$ is conjugate with a structurally stable smooth flow on T—again denoted by $\mathcal{X}(\mathcal{G})$—with as equilibria: $2r$ star nodes (r of them being stable, the other r unstable) and $2r$ orthogonal saddles. The underlying "distinguished graph" is denoted again by $\mathcal{G}$. It follows that the angle between two $\mathcal{G}$-edges (i.e. unstable separatrices at saddles for $\mathcal{X}(\mathcal{G})$) that are incident with the same $\mathcal{G}$-vertex (i.e. a stable star node for $\mathcal{X}(\mathcal{G})$), may assumed to be well defined and non-vanishing.

We adopt the notations/conventions as introduced in the preambule to Definition 3.7 (*A-property*). In particular, let the $\mathcal{G}$-vertex v_i stand for a stable node of $\mathcal{X}(\mathcal{G})$. In Fig. 18 (a) we present a picture of $\mathcal{X}(\mathcal{G})$ w.r.t. the $\mathbf{y}$-coordinates around $\mathbf{0}$ $(= v_i)$. Here the bold lines stand for $\mathcal{G}$-edges, and the thin lines for other $\mathcal{X}(\mathcal{G})$-trajectories on a small disk D around $\mathbf{y} = \mathbf{0}$. Note that the angles $\omega_{i(k)}$ in this figure fulfil the conditions (A_1), (A_2) of Definition 3.7. In Fig. 18 (b), we consider a similar configuration of $\mathcal{X}(\mathcal{G})$-trajectories on D approaching v_i, with the only additional condition that the tuples $(e_{i(1)}, \ldots, e_{i(\delta_i)})$ and $(e'_{i(1)}, \ldots, e'_{i(\delta_i)})$ are equally ordered. Consider the oriented arcs $\mathrm{arc}(i(k), i(k+1))$ and $\mathrm{arc}'(i(k), i(k+1))$ in the boundary ∂D of D, determined by respectively the consecutive pairs $(e_{i(k)}, e_{i(k+1)})$ and $(e'_{i(k)}, e'_{i(k+1)})$. Under suitable shrinking/stretching, these arcs can be identified. This yields an orientation preserving homeomorphism ψ from ∂D onto itself. It is easily proved that ψ can be extended to a homeomorphism $\Psi : D \to D$ mapping the $\mathcal{X}(\mathcal{G})$-trajectories in Fig. 18 (a) onto those in Fig. 18 (b). This procedure will be referred to as a local re-drawing (around v_i).

With the aid of local re-drawings, together with a "cut" and "paste" construction, the pair $(\mathcal{X}(\mathcal{G}), \mathcal{G})$ can be changed into an equivalent structurally stable flow (again denoted $\mathcal{X}(\mathcal{G})$) and an equivalent distinguished graph (again denoted $\mathcal{G}$), with pictures as Fig. 18 (b) instead of Fig. 18 (a). We conclude that the angles $\omega_i(k)$ in Fig. 18 (a) may be altered arbitrarily (provided that conditions (A_1), (A_2) of Definition 3.7 persist) without changing the topological types of $\mathcal{X}(\mathcal{G})$ and $\mathcal{G}$.

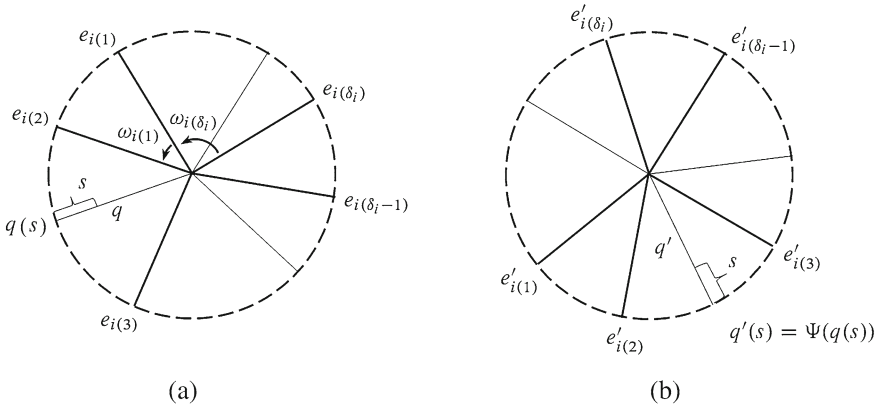

Fig. 18 Local phase portraits of $\mathcal{X}(\mathcal{G})$ around a stable star node before and after local re-drawing

Note that any toroidal graph, equivalent with a Newton graph (such as the original graph $\mathcal{G}$), is also a Newton graph (cf. Definition 3.1, Lemma 3.11). Moreover, not only $\mathcal{G}$, but also $\mathcal{G}^*$ is Newtonian (cf. Lemma 3.14). Hence, compare (the proof of) Lemma 3.15, with the aid of local re-drawings around the vertices of $\mathcal{G}$ and $\mathcal{G}^*$, together with a "cut and past construction", it is easily shown that: in each face of $\mathcal{G} \wedge \mathcal{G}^*$ (canonical $\mathcal{X}(\mathcal{G})$-region), the angles at the $\mathcal{G}$- and $\mathcal{G}^*$-vertex (a stable, respectively unstable, star node of $\mathcal{X}(\mathcal{G})$) are equal and non-vanishing.

With respect to the various local $\mathbf{y}$-coordinate systems around the $\mathcal{X}(\mathcal{G})$-equilibria, we define the $4r$ functions h_i, h_i^*, h_j^{**}, $i = 1, \ldots, r$, $j = 1, \ldots, 2r$, as follows:

$$
\begin{aligned}
h_i(\mathbf{y}) &= \frac{1}{2}(y_1^2 + y_2^2) && \text{in case of stable nodes at } \mathbf{y} = \mathbf{0} \\
& && \text{representing the } r \text{ vertices } v_i \text{ of } \mathcal{G}, \\
h_i^*(\mathbf{y}) &= -\frac{1}{2}(y_1^2 + y_2^2) && \text{in case of unstable nodes at } \mathbf{y} = \mathbf{0} \\
& && \text{representing the } r \text{ vertices } v_i^* \text{ of } \mathcal{G}^*, \\
h_j^{**}(\mathbf{y}) &= \frac{1}{2}(y_1^2 - y_2^2) && \text{in case of saddles at } \mathbf{y} = \mathbf{0} \\
& && \text{representing the } 2r \text{ edges } e_j \text{ of } \mathcal{G}.
\end{aligned}
$$

Note that each function exhibits a non-degenerate critical point at $\mathbf{y} = \mathbf{0}$. Moreover, on a $\mathbf{y}$-coordinate neighborhood N around an equilibrium of $\mathcal{X}(\mathcal{G})$, the vector field $\mathcal{X}(\mathcal{G})$ is the negative gradient vector field [w.r.t. the standard Riemannian structure on N] of the associated function. Apparently, the flow $\mathcal{X}(\mathcal{G})$, being structurally stable on T (without limit cycles), together with the functions h_i, h_i^* and h_j^{**}, fulfils the requirements (1)–(4) laid upon [21, Theorem B]. So, applying this theorem we may conclude that there is a function h on T such that:

1. The critical points of h coincide with the equilibria of $\mathcal{X}(\mathcal{G})$ and h coincides with the functions h_i, h_i^*, h_j^{**} plus a constant in some neighborhood of each critical point.
2. $Dh(x) \cdot \mathcal{X}(\mathcal{G})|_x < 0$ outside the critical point set $\mathrm{Crit}(h)$ of h.

3. The function h is *self-indexing*, i.e., the value of h in a critical point β equals the Morse index of $\beta = \#(\text{negative eigenvalues of } D^2h(\beta))$. Thus, $h(\beta) = 0\,(=2)$, in case of a stable (unstable) node and $h(\beta) = 1$ in case of a saddle.

As a corollary (cf. [13, Theorem 8.2.8] and [21]), we conclude that there is a variable (Riemannian) metric $R(\cdot)$ on T such that

$$\operatorname{grad}_R h = \mathcal{X}(\mathcal{G}),$$

where $\operatorname{grad}_R h$ is a vector field on T of the form (w.r.t. local coordinates $\mathbf{x}$ for T)

$$\operatorname{grad}_R h(\mathbf{x}) = -R^{-1}(\mathbf{x})\, D^{\mathrm{T}} h(\mathbf{x}).$$

Here $R(\mathbf{x})$ is a symmetric, positive definite 2×2-matrix with coefficients depending in a C^1-fashion on $\mathbf{x}$. Note that the direction of $\operatorname{grad}_R h$ is uniquely determined by the above transversality condition 2, whereas on the neighborhoods N around the $\mathcal{X}(\mathcal{G})$-equilibria, the matrices $R(\cdot)$ are just the 2×2-unit matrix I_2. Moreover, $\operatorname{grad}_R h(\mathbf{x}) \neq 0$ if and only if $\mathbf{x}$ is outside the set $\operatorname{Crit}(h)$ (= set of $\mathcal{X}(\mathcal{G})$ − equilibria).

For $\mathbf{x} \notin \operatorname{Crit}(h)$, let $\operatorname{grad}^{\perp}_{R(\mathbf{x})} h(\mathbf{x}) \neq 0$, be a vector R-orthogonal to $\operatorname{grad}_{R(\mathbf{x})} h(\mathbf{x})$, i.e.

$$(\operatorname{grad}^{\perp}_{R(\mathbf{x})} h(\mathbf{x}))^{\mathrm{T}} . R(\mathbf{x}) . (-R^{-1}(\mathbf{x}) . D^{\mathrm{T}} h(\mathbf{x}))\ [= -Dh(\mathbf{x}) . \operatorname{grad}^{\perp}_{R(\mathbf{x})} h(\mathbf{x})] = 0. \quad (10)$$

Let x_0 be a point in the level set $L_c = \{x \in T : h(x) = c,\ c = \text{constant}\}$. Then we have:

- Assume $x_0 \notin \operatorname{Crit}(h)$, thus L_c is, locally around x_0, a regular curve. By (10), this local curve is R-orthogonal to the trajectory of $\mathcal{X}(\mathcal{G})$ $(=\operatorname{grad}_R h)$ through x_0.
- If $x_0 \in \operatorname{Crit}(h)$, then x_0 is either an isolated point, surrounded by closed regular curves L_c, $c \neq 0, 2$ (in the case where x_0 is a $\mathcal{X}(\mathcal{G})$-node), or a ramification point at the intersection of two (orthogonal) components of L_1 (in case of a $\mathcal{X}(\mathcal{G})$-saddle). This follows from the fact that on the neighborhoods N around the equilibria of $\mathcal{X}(\mathcal{G})$, the Riemannian metric R is just the standard one.

So, we may subdivide the level sets L_c into the disjunct union of maximal regular curves (to be referred to as to the level lines L_c) and single points (in $\operatorname{Crit}(h)$). Let $\mathbf{x}(t)$, $\mathbf{x}(0) \notin \operatorname{Crit}(h)$ be a trajectory for $\mathcal{X}(\mathcal{G})$ $(=\operatorname{grad}_R h)$. Since $R^{-1}(\mathbf{x})$ is a symmetric, positive definite matrix, we have

$$\begin{aligned} \frac{d}{dt} h(\mathbf{x}(t))|_{t=0} &= Dh(\mathbf{x}(0)) \cdot \mathbf{x}'(0) \\ &= Dh(\mathbf{x}(0)) \cdot (-R^{-1}(\mathbf{x}(0))) \cdot D^{\mathrm{T}} h(\mathbf{x}(0)) < 0. \end{aligned} \quad (11)$$

So, $h(\mathbf{x}(t))$ decreases when t increases, and by the indexing condition 3, $0 \leqslant h(x) \leqslant 2$, for all $x \in T$. By (11), when travelling along the boundary of an open canonical $\mathcal{X}(\mathcal{G})$-region $[= \mathcal{G} \wedge \mathcal{G}^* - \text{face}]$, say $\overline{\overline{\mathcal{R}}}_{ij}$ in Fig. 19, the functional values of h vary strictly from 2 (at the unstable node v_j^*) via 1 (at a saddle σ_1 or σ_2) to 0 (at the stable node

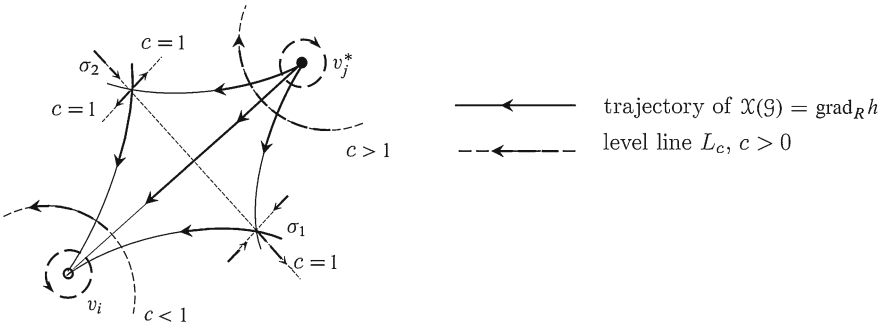

Fig. 19 The canonical $\mathcal{X}(\mathcal{G})$-region $\overline{\overline{\mathcal{R}}}_{ij}$

v_i). From this it follows (use also the transversality condition 2.) that a level line L_c, entering $\overline{\overline{\mathcal{R}}}_{ij}$ through the boundary $\partial\overline{\overline{\mathcal{R}}}_{ij}$ between v_i and σ_1 [thus $0 < c < 1$], must leave this region through $\partial\overline{\overline{\mathcal{R}}}_{ij}$ between v_i and σ_2. Also, if L_c enters $\overline{\overline{\mathcal{R}}}_{ij}$ through $\partial\overline{\overline{\mathcal{R}}}_{ij}$ between v_j^* and σ_1 [thus $1 < c < 2$], then it leaves $\overline{\overline{\mathcal{R}}}_{ij}$ through $\partial\overline{\overline{\mathcal{R}}}_{ij}$ between v_j^* and σ_2. By the same argumentation, the saddles σ_1 and σ_2 are connected by a level line L_1. Considering unions of all $\mathcal{G} \wedge \mathcal{G}^*$-faces incident with the same vertex representing a stable (unstable) attractor of $\mathcal{X}(\mathcal{G})$, we find that the level sets L_c, $c \neq 0, 1$ or 2, are closed smooth regular curves, either contractable to a stable attractor [in case $0 < c < 1$], or to an unstable attractor [in case $1 < c < 2$] . Altogether, a level line L_c is either a closed curve, or it connects two different $\mathcal{X}(\mathcal{G})$-saddles. Hence, the following definition makes sense (compare also Definition 2.18):

Definition 4.2 The graph $\mathcal{G}^\perp$ on the torus T is given by:

- Vertices are the $2r$ saddles for $\mathcal{X}(\mathcal{G})$ on T.
- Edges are the $4r$ level lines L_1 connecting different saddles of $\mathcal{X}(\mathcal{G})$.

Apparently, $\mathcal{G}^\perp$ is cellularly embedded, and, by Euler's formula, this graph is connected (since there are $2r$ faces, determined by the stable and unstable nodes of $\mathcal{X}(\mathcal{G})$). So, the function h admits the same value on (the edges and vertices of) $\mathcal{G}^\perp$, whereas, by the self-indexing condition 3, we know that this value equals 1. Thus, the embedded graph $\mathcal{G}^\perp$, as a point set in T, is just the level set L_1. This leads to Fig. 20, where we present the graphs $\mathcal{G}$, $\mathcal{G}^*$ and $\mathcal{G}^\perp$, together with some more level lines L_c. We endow the level lines L_c, $0 < c < 1$ (the level lines L_c, $1 < c < 2$) with the anti-clockwise (clock-wise) orientation. Doing so, we can turn $\mathcal{G}^\perp$ into an oriented graph; see Fig. 20.

We fix the vector field $\mathrm{grad}^\perp_{R(\mathbf{x})} h(\mathbf{x})$ by demanding that it has the same length as $\mathrm{grad}_R h(\mathbf{x})$ (w.r.t. the norm, induced by $R(\mathbf{x})$) and is oriented according to the orientation of the level line L_c through $\mathbf{x}$, see Fig. 19. So, by (10), we may interpret the net of $\mathcal{X}(\mathcal{G})$-trajectories and level lines L_c as the R-orthogonal net of trajectories for the vector fields $\mathrm{grad}_R h$ and $\mathrm{grad}^\perp_R h$. The switch from $\mathcal{X}(\mathcal{G})$ to $\mathcal{X}(\mathcal{G}^*)$ $(= -\mathcal{X}(\mathcal{G}))$ causes the reverse of the orientations in this net. So, for the open canonical regions of $\mathcal{X}(\mathcal{G})$ and $\mathcal{X}(\mathcal{G}^*)$, we have $\overline{\overline{\mathcal{R}}}_{ij} = \overline{\overline{\mathcal{R}}}^*_{ji}$ (as point sets). However, the role of v_i and v_j^*,

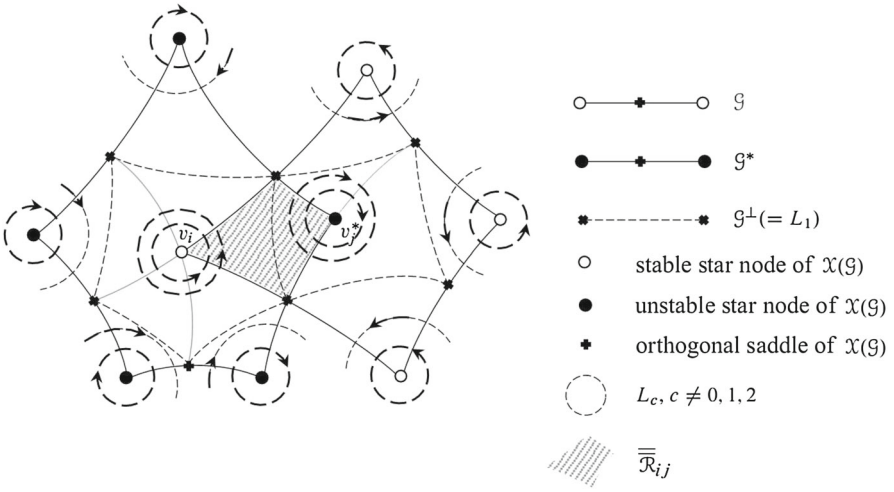

Fig. 20 The graphs $\mathcal{G} \wedge \mathcal{G}^*$, $\mathcal{G}^\perp$ and some level sets for h

and of σ_1 and σ_2 (w.r.t. the orientations of the trajectories) is exchanged, see Fig. 21, where the equal angles at v_i and v_j^* in $\overline{\overline{\mathcal{R}}}_{ij}$ and $\overline{\overline{\mathcal{R}}}^*_{ji}$ are denoted by α.

Reasoning as in the case of the function h for $\mathcal{X}(\mathcal{G})$, we find a self-indexing smooth function, say g, for $\mathcal{X}(\mathcal{G}^*)$ with the following property: when traveling along the boundary of $\overline{\overline{\mathcal{R}}}^*_{ji}$, the functional values of g vary strictly from 2 (at the unstable node v_i) via 1 (at a saddle σ_1 or σ_2) to 0 (at the stable node v_j^*).

Consider an arbitrary $\mathcal{X}(\mathcal{G})$-trajectory, say γ_Δ, in $\overline{\overline{\mathcal{R}}}_{ij}$, approaching v_i under a positive angle Δ with the $\mathcal{G}$-edge $(= \mathcal{X}(\mathcal{G})$-trajectory$)$ $v_i\sigma_1$; see Fig. 21. The set of all such trajectories is parametrized by the values of Δ in the interval $(0, \alpha)$ and the functional values of h (or g) on $\overline{\overline{\mathcal{R}}}_{ij}$. We map γ_Δ onto the half ray $r(x)\exp(i\Delta)$, $x \in \gamma_\Delta$, where

$$r(x) = h(x), \qquad \text{if } x \text{ is on } \gamma_\Delta \text{ between } v_i \text{ and } p \ (= \text{intersection } \gamma_\Delta \cap L_1),$$
$$r(x) = \frac{1}{g(x)}, \qquad \text{if } x \text{ is on } \gamma_\Delta \text{ between } p \text{ and } v_j^*.$$

In this way, the R-orthogonal net of trajectories for $\mathcal{X}(\mathcal{G})$ $(= \text{grad}_R h)$ and $\text{grad}_R^\perp h$ on $\overline{\overline{\mathcal{R}}}_{ij}$ can be homeomorphically mapped onto the polar net on the open sector, say $s(\overline{\overline{\mathcal{R}}}_{ij})$, in the complex plane as in Fig. 22 (a). Here 0 corresponds to v_i, and σ_1', σ_2' (both situated on the unit circle) are related to respectively σ_1 and σ_2.

Similarly, the trajectory $\gamma^*_{\Delta^*}$ in $\overline{\overline{\mathcal{R}}}^*_{ji}$ can be mapped onto the half ray $\exp(i\Delta^*)/r(x)$, $x \in \gamma^*_{\Delta^*}$, where Δ^* is the angle at v_j^* between this trajectory and the $\mathcal{G}^*$-edge $v_j^*\sigma_1$, see Fig. 21, where $\Delta^* = \Delta$ (apart from orientation). Hence, the R-orthogonal net of trajectories for $\mathcal{X}(\mathcal{G}^*)$ $(= -\text{grad}_R h)$ and $-\text{grad}_R^\perp h$ on $\overline{\overline{\mathcal{R}}}^*_{ji}$ can be homeomorphically mapped onto the polar net on the sector, obtained from $s(\overline{\overline{\mathcal{R}}}_{ij})$ by reflection in

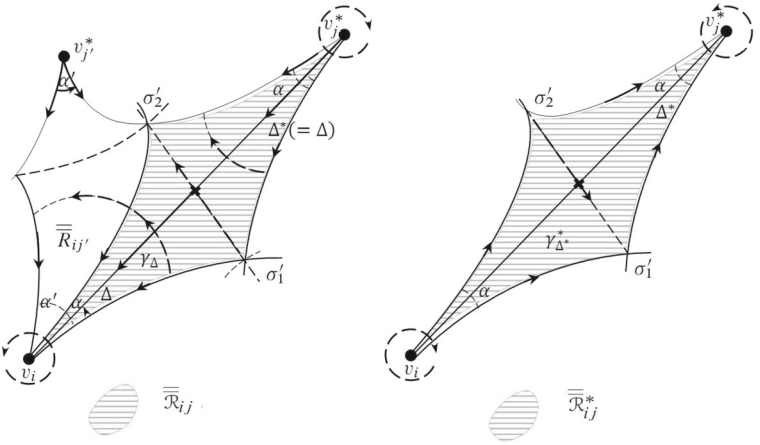

Fig. 21 $\overline{\overline{\mathcal{R}}}_{ij}$ and $\overline{\overline{\mathcal{R}}}_{ij}^*$

the real axis. We call this sector $S(\overline{\overline{\mathcal{R}}}_{ji}^*)$. Here 0 corresponds to v_j^*, and $(\sigma_1^*)'$, $(\sigma_2^*)'$ (both situated on the unit circle) are related to respectively σ_1 and σ_2. Reversing the orientations of the polar net in the latter section, we obtain a polar net, oriented as the $\mathcal{X}(\mathcal{G})$ $(=\text{grad}_R h)$ and $\text{grad}\frac{1}{R}^{\perp} h$-trajectories on $\overline{\overline{\mathcal{R}}}_{ij}$. Endowed with this polar net we rename $S(\overline{\overline{\mathcal{R}}}_{ji}^*)$ as $S(\overline{\overline{\mathcal{R}}}_{ij})$. Apparently, the polar nets on $s(\overline{\overline{\mathcal{R}}}_{ij})$ and $S(\overline{\overline{\mathcal{R}}}_{ij})$ correspond under the inversion $z \to 1/z$. Compare Fig. 22 (a), (b). In the same way, we map a neighbouring region $\overline{\overline{\mathcal{R}}}_{ij'}$ as in Fig. 21, homeomorphically onto the sector $s(\overline{\overline{\mathcal{R}}}_{ij'})$ in Fig. 22 (a) and also onto $S(\overline{\overline{\mathcal{R}}}_{ij'})$ in Fig. 22 (c). Repeating this procedure we are able to map all canonical regions of $\mathcal{X}(\mathcal{G})$ onto (the closures of) sectors of the types $s(\cdot)$ and $S(\cdot)$ in such a way that together they cover, for each value of i and j, a copy of the complex plane (compare also Figs. 11, 12).

In analogy with Remark 2.20, we consider the reduced torus $\check{T} = T \backslash \{\mathcal{G} \wedge \mathcal{G}^*\text{-vertices}\}$, and on $\check{T}$ the covering by open neighborhoods

$$\{F_{v_i}^* \backslash v_i,\, F_{v_j^*} \backslash v_j^*\}, \qquad i, j = 1, \ldots, r,$$

where $F_{v_i}^*$ and $F_{v_j^*}$ stand for the basins of $\mathcal{X}(\mathcal{G})$ for respectively v_i and v_j^*. Again, only intersections of the type $(F_{v_i}^* \backslash v_i) \cap (F_{v_j^*} \backslash v_j^*)$ are possibly non-empty. Even so, such an intersection consists of the disjoint union of regions of the type $\overline{\overline{\mathcal{R}}}_{ij}$, say $\overline{\overline{\mathcal{R}}}_{ij}^1, \ldots, \overline{\overline{\mathcal{R}}}_{ij}^s$, where s is the amount of vertices v_i (vertices v_j^*) in the Π-walks of $F_{v_j^*}$ (of $F_{v_i}^*$). Note that at v_i, respectively v_j^*, these regions $\overline{\overline{\mathcal{R}}}_{ij}^k$ are endowed with the anti-clockwise (clockwise) cyclic orientation, and are separated by regions not of this type; compare Remark 2.8 and Sect. 3.2.

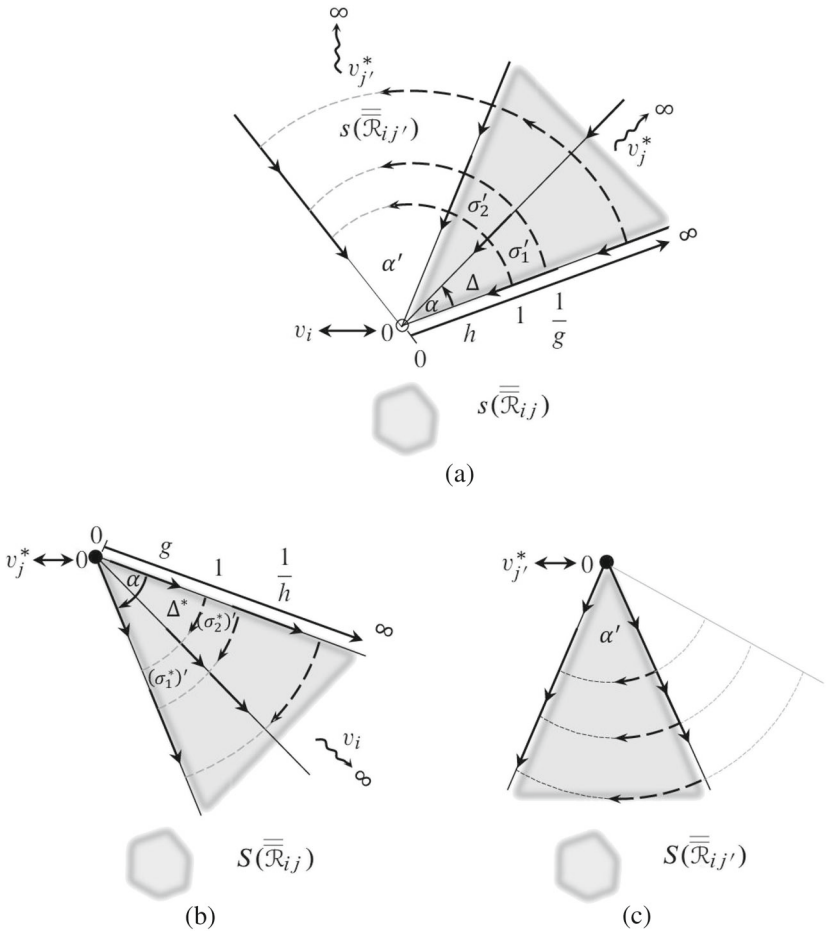

Fig. 22 $s(\overline{\overline{\mathcal{R}}}_{ij})$, $S(\overline{\overline{\mathcal{R}}}_{ij})$ and $s(\overline{\overline{\mathcal{R}}}_{ij'})$, $S(\overline{\overline{\mathcal{R}}}_{ij'})$

Now, we proceed as in Remark 2.20. The open covering of $\check{T}$ provides this manifold with a complex analytic structure, exhibiting coordinate transformations

$$s(\overline{\overline{\mathcal{R}}}_{ij}^k) \leftrightarrow S(\overline{\overline{\mathcal{R}}}_{ij}^k), \qquad i, j = 1, \ldots, r,$$

induced by the inversion $z \to 1/z$. We pull back the restrictions of the function z (respectively $1/z$) on the various sectors $s(\overline{\overline{\mathcal{R}}}_{ij}^k)$, respectively $S(\overline{\overline{\mathcal{R}}}_{ij}^k)$ to $\check{T}$. By glueing all canonical regions for $\mathcal{X}(\mathcal{G})$ along the trajectories in their common boundaries, we construct a complex analytic function on $\check{T}$. Continuous extension to T yields a meromorphic function, say f on T, with r simple zeros (poles) at v_i (v_j^*) and $2r$ simple saddles at $\sigma_1, \ldots, \sigma_{2r}$. Since $\overline{\mathcal{N}}(z) = -z$, $\overline{\mathcal{N}}(1/z) = -1/z$, we find $\mathcal{X}(\mathcal{G}) = \overline{\overline{\mathcal{N}}}(f)$, thus $\mathcal{G} = \mathcal{G}(f)$. This proves Theorem 4.1.

We combine this result together with the results in Theorem 2.10 and Corollary 3.16 to obtain:

Theorem 4.3 (Representation of structurally stable elliptic Newton flows by graphs) *Up to conjugacy* ($\sim$) *between flows and equivalency* ($\sim$) *between graphs, the structurally stable Newton flows of* r^{th} *order are 1-1 represented by the Newton graphs of order* r.

5 Final remarks

5.1 Rational versus elliptic Newton flows

Our study is inspired by the analogy between rational and elliptic functions. We raised the question whether, and (even so) to what extent, this analogy persists in terms of the corresponding Newton flows (on, respectively, the Riemann sphere S^2 and the torus T). An affirmative answer to this question is given by comparing the *characterization, genericity, classification and representation aspects* of rational Newton flows (see [8, Theorem 2.1]) with their counterparts as described in Theorems 1.3, 2.10 and 4.3.

More in particular, this analogy becomes manifest when we look at the special case of *balanced rational* Newton flows of order $r \geqslant 1$. By these, we mean structurally stable flows of the form $\overline{\overline{\mathcal{N}}}(p_n/q_m)$, with p_n, q_m two co-prime polynomials of degrees respectively n, m, $|n-m| \leqslant 1$, $r = \max\{n, m\}$. Such flows admit $2r$ star nodes (r stable and r unstable) together with $2r-2$ orthogonal saddles. [Note that at $z = \infty$ (north pole) there is an unstable node if $n = m+1$, a stable node if $m = n+1$, and a saddle if $m = n$.] Due to the duality property,[17] the transition $p_n/q_m \leftrightarrow q_m/p_n$ causes the reverse of orientations of the trajectories of $\overline{\overline{\mathcal{N}}}(p_n/q_m)$ and $\overline{\overline{\mathcal{N}}}(q_m/p_n)$. So, these flows may be considered as equal and we assume $n \geqslant m$. Now, the oriented sphere graph $G(p_n/q_m)$ for $\overline{\overline{\mathcal{N}}}(p_n/q_m)$ can be defined (in strict analogy with Definition 2.1) as a connected, cellularly embedded multigraph with r vertices, $2r-2$ edges and r faces; apparently, also $G(q_m/p_n) = -G^*(p_n/q_m)$ holds. As in the elliptic case, it can be proved that $G(p_n/q_m)$ fulfils both the E- and the A-property. (However, in this special case it is found that the later property already implies the first one.) Subsequently, it is shown that any cellularly embedded multigraph in S^2 with r vertices, $2r-2$ edges and r faces, admits the A-property iff certain (Hall) inequalities are satisfied. Altogether, this leads to a concept of Newton graph that is formally the same as the concept of Newton graph in Definition 3.13. In particular, classification and representation results, similar to Theorems 2.10 and 4.3, are derived (cf. [11, 12]).

We conclude that there is a striking analogy between the balanced Newton flows and elliptic Newton flows, both of order r. Note that an elliptic Newton flow of order 1 is not defined, whereas a balanced Newton flow of order 1 is just the North–South flow (cf. [8, Figs. 7, 8] for $n = 1$).

[17] Duality for rational Newton flows is easily verified, see (1).

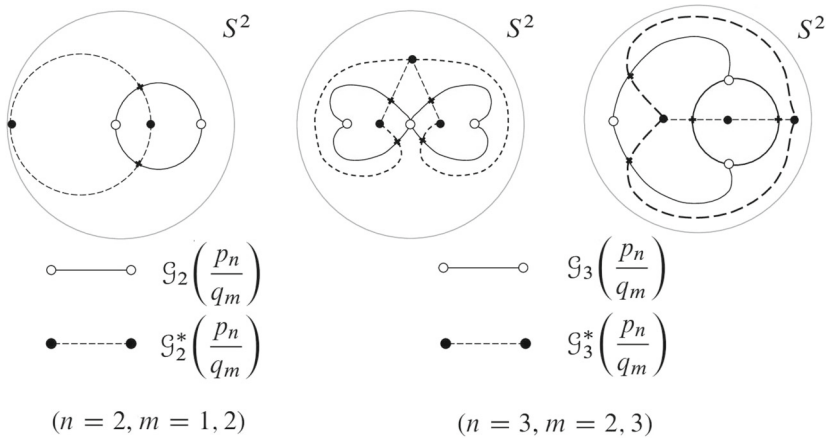

Fig. 23 The different graphs for balanced rational Newton flows of order $r = 2, 3$

Finally, we note that, as in the elliptic case, for lower values of r a list of all possible (up to conjugacy and duality) balanced Newton flows, represented by their graphs, is available. For example, see Fig. 23, where the pictures of the graphs $G_r(p_n/q_m)$ and $G_r^*(p_n/q_m)$, $r = 2, 3$, suggest that the conditions (A_1)–(A_3) of Definition 3.7 are indeed fulfilled. The proof that these graphs are the only possibilities, based on the Representation Theorem for rational Newton flows (compare [11]), is omitted.

5.2 Complexity aspects

We indicate the existence of a "good" (i.e., polynomial) algorithm deciding whether a given cellularly embedded toroidal graph $\mathcal{G}_r$ is a Newton graph or not. To this aim, we check both the E- and A-property.

E-property: Use that the graphs (facial walks) ∂F_j are Eulerian iff all vertices have even degree.

A-property: Let B be a finite bipartite graph with bipartition (X, Y), and denote for any subset S in X the neighbour set in Y by $N(S)$. We consider the so-called Strong Hall Property (cf. [4]):

$$|S| < |N(S)| \qquad \text{for all non-empty } S \subset X. \tag{12}$$

For each *bipartite* graph, obtained from (B, X, Y) by adding one vertex (p) to X and one edge which joins p to a Y-vertex, we also consider the Hall property (cf. [3]):

$$|\check{S}| \leqslant |N(\check{S})| \qquad \text{for all subsets } \check{S} \text{ of } X \cup \{p\}. \tag{13}$$

It is easily shown that (12) and (13) are equivalent, and thus, because the verification of (13) is possible in polynomial time (cf. [3]), this is also true for (12). Now, we

select an arbitrary $\mathcal{G}_r$-face F_j, say F_r, and specify (B, X, Y) by $X = \{F_1, \ldots, F_{r-1}\}$. $Y = V(\mathcal{G}_r)$, where adjacency is defined by inclusion. The inequalities in the r.h.s. of Lemma 3.11 take the form (12) for all non-empty J in $\{1, \ldots, r-1\}$, and considering all possible choices for F_j, we are done.

References

1. Abramowitz, A., Stegun, I.A. (eds.): Handbook of Mathematical Functions. Dover Books on Mathematics. Dover, New York (1965)
2. Andronov, A.A., Leontovich, E.A., Gordon, I.I., Maier, A.G.: Theory of Bifurcations of Dynamical Systems on a Plane. Israel Program for Scientific Translations, Jerusalem (1973)
3. Bondy, J.A., Murty, U.S.R.: Graph Theory with Applications. American Elsevier, New York (1976)
4. Coleman, T.F., Edenbrandt, A., Gilbert, J.R.: Predicting fill for sparse orthogonal factorization. J. Assoc. Comput. Mach. **33**(3), 517–532 (1986)
5. Giblin, P.J.: Graphs, Surfaces and Homology. Chapman and Hall Mathematics Series. Chapman and Hall, London (1977)
6. Harary, F.: Graph Theory. Addison-Wesley, Reading (1969)
7. Hartman, P.: Ordinary Differential Equations. Birkhäuser, Boston (1982) (Reprint of the 2nd edn.)
8. Helminck, G.F., Twilt, F.: Newton flows for elliptic functions I. Structural stability: characterization & genericity (2016). arXiv:1609.01267v2
9. Helminck, G.F., Twilt, F.: Newton flows for elliptic functions III. Classification of 3rd order Newton graphs (2016). arXiv:1609.01335v1
10. Jongen, H.Th., Jonker, P., Twilt, F.: The continuous Newton-method for meromorphic functions. In: Martini, R. (ed.) Geometric Approaches to Differential Equations. Lecture Notes in Mathematics, vol. 810, pp. 181–239. Springer, Berlin (1980)
11. Jongen, H.Th., Jonker, P., Twilt, F.: The continuous, desingularized Newton method for meromorphic functions. Acta Appl. Math. **13**(1–2), 81–121 (1988)
12. Jongen, H.Th., Jonker, P., Twilt, F.: On the classification of plane graphs representing structurally stable rational Newton flows. J. Combin. Theory Ser. B **51**(2), 256–270 (1991)
13. Jongen, H.Th., Jonker, P., Twilt, F.: Nonlinear Optimization in Finite Dimensions. Nonconvex Optimization and Its Applications, vol. 47. Kluwer, Dordrecht (2000)
14. Mangasarian, O.L.: Nonlinear Programming. McGraw-Hill, New York (1969)
15. Markushevich, A.I.: Theory of Functions of a Complex Variable, vol. II. Prentice Hall, Englewood Cliffs (1965)
16. Markushevich, A.I.: Theory of Functions of a Complex Variable, vol. III. Prentice Hall, Englewood Cliffs (1967)
17. Mirsky, L.: Transversal Theory. Mathematics in Science and Engineering, vol. 75. Academic Press, New York (1971)
18. Mohar, B., Thomassen, C.: Graphs on Surfaces. John Hopkins Studies in the Mathematical Sciences. John Hopkins University Press, Baltimore (2001)
19. Peixoto, M.M.: Structural stability on two-dimensional manifolds. Topology **1**(2), 101–120 (1962)
20. Peixoto, M.M.: On the classification of flows on 2-manifolds. In: Peixoto, M.M. (ed.) Dynamical Systems, pp. 389–419. Academic Press, New York (1973)
21. Smale, S.: On gradient dynamical systems. Ann. Math. **74**(1), 199–206 (1961)
22. Twilt, F., Helminck, G.F., Snuverink, M., van den Burg, L.: Newton flows for elliptic functions: a pilot study. Optimization **57**(1), 113–134 (2008)